



**Università degli Studi di Milano**

---

**FACOLTÀ DI SCIENZE E TECNOLOGIE**  
**CORSO DI LAUREA IN FISICA**

**TESI DI LAUREA TRIENNALE**

**Coulombic interactions in the fractional  
quantum Hall effect: from three particles  
to the many-body approach**

Candidato:  
**Daniele Oriani**  
Matricola 828482

Relatore:  
**Prof. Luca Guido Molinari**

This page intentionally left blank.

# Contents

<b>Abstract</b>	<b>5</b>
<b>1 Uncorrelated electrons in uniform magnetic field</b>	<b>7</b>
1.1 Overview of Hall effects . . . . .	7
1.2 Landau levels . . . . .	9
1.2.1 Energy spectrum . . . . .	9
1.2.2 Degeneracy . . . . .	10
1.2.3 Bargmann space . . . . .	12
1.2.4 Eigenfunctions . . . . .	14
1.3 Integer Quantum Hall Effect . . . . .	16
<b>2 Fractional quantum Hall effect</b>	<b>19</b>
2.1 Conceptual framework . . . . .	19
2.2 Exact solution for the three particle problem . . . . .	21
2.2.1 Two interacting particles . . . . .	21
2.2.2 Three interacting particles . . . . .	23
2.3 Many-body framework . . . . .	30
2.3.1 The hamiltonian . . . . .	30
2.3.2 Laughlin's ansatz . . . . .	31
<b>3 Coulomb interaction in the disk geometry</b>	<b>35</b>
3.1 System geometry . . . . .	35
3.2 Analytic Coulomb interaction matrix elements . . . . .	37
3.3 Exact diagonalization for finite cluster . . . . .	41
3.3.1 Framework . . . . .	42
3.3.2 Numerical study . . . . .	46
3.3.3 Remarks . . . . .	50
<b>Conclusions</b>	<b>53</b>
<b>A Three particles matrix elements</b>	<b>55</b>
<b>References</b>	<b>59</b>

This page intentionally left blank.

# Abstract

Since its discovery in 1982 by Tsui, Stormer and Gossard [1] the fractional quantum Hall effect has piqued the interest of physicists, notably because of the extreme correlation properties emerging in the system.

In the wake of the discovery of the plateau at filling factor  $1/3$ , R.B. Laughlin published some pioneering works in an effort to provide the phenomenon with a theoretical explanation: he started by studying the problem of three interacting electrons with first-quantized formalism [2] and then moved on to proposing an extremely successful ansatz for the ground state [3] by guessing it from general assumptions.

Nonetheless, the reason why Laughlin's wavefunction approximates the true ground state so well is still unknown. Current efforts aim to answer this question, for example by studying the expansion of the ansatz in Slater determinants [4][5], as well as to provide alternative, more general theories (such as Composite Fermion theory [6]) that are able to describe all of the observed plateaux in a unified fashion.

In this thesis we solve the three particle problem exactly, which gives us physical insight in our review of the many-body problem. In the third chapter we study the effect in the disk geometry, by performing the exact diagonalization of the hamiltonian. Finally we compare our exact ground states for small clusters of electrons with Laughlin's ansatz, obtained from its expansion in Slater determinants.

This page intentionally left blank.

# Chapter 1

## Uncorrelated electrons in uniform magnetic field

### 1.1 Overview of Hall effects

Consider a conducting material in which there are an electric field  $\mathbf{E}$  and a magnetic field  $\mathbf{B}$ , both static in time and homogeneous in space. Let their directions be orthogonal and fix a reference frame so that  $\mathbf{E} = E \hat{\mathbf{x}}$  and  $\mathbf{B} = B \hat{\mathbf{z}}$ . Then the electrons in the material will flow in the  $\hat{\mathbf{y}}$  direction, giving rise to a current. This is the Hall effect, first accounted in 1879 [7].

In the aforementioned conditions a point charge  $q$  of mass  $m$  obeys the classical equation of motion

$$m\ddot{\mathbf{x}} = q \left( \mathbf{E} + \frac{\dot{\mathbf{x}}}{c} \times \mathbf{B} \right) \quad (1.1.1)$$

If we suppose the current to be stationary this quantity is zero. Moreover, if  $\mathbf{J} = q\rho_0\dot{\mathbf{x}}$  is the current density and  $\rho_0$  is the density of the point charges in the material, Ohm's law reads

$$\mathbf{E} = \hat{\boldsymbol{\rho}} \mathbf{J} = q\rho_0 \hat{\boldsymbol{\rho}} \dot{\mathbf{x}}, \quad (1.1.2)$$

where  $\hat{\boldsymbol{\rho}}$  is the resistivity tensor. Substituting in the equation of motion (1.1.1) gives

$$\rho_{ij} = -\text{sgn}(q)\epsilon_{ij3} \rho_H \quad \rho_H := \frac{B}{|q|c\rho_0} \quad (1.1.3)$$

The quantity  $\rho_H$  is called Hall resistivity. In this setup the diagonal resistivity  $\rho_{ii}$  is vanishing and the charges, which from now we will consider to be electrons of charge  $q = -e$ , have a velocity perpendicular to both fields. In passing, we observe that in the case of a two dimensional conductor resistance and resistivity are exactly the same quantity and thus we can speak equivalently of Hall resistance or Hall resistivity:  $R_H \equiv \rho_H$ .

## 1. UNCORRELATED ELECTRONS IN UNIFORM MAGNETIC FIELD

This result for the Hall resistance is in complete agreement with that of Drude's model for transport phenomena in conductors. However, they both hold only in the case of weak magnetic fields. As  $B$  is increased quantum mechanical effects begin to be apparent.

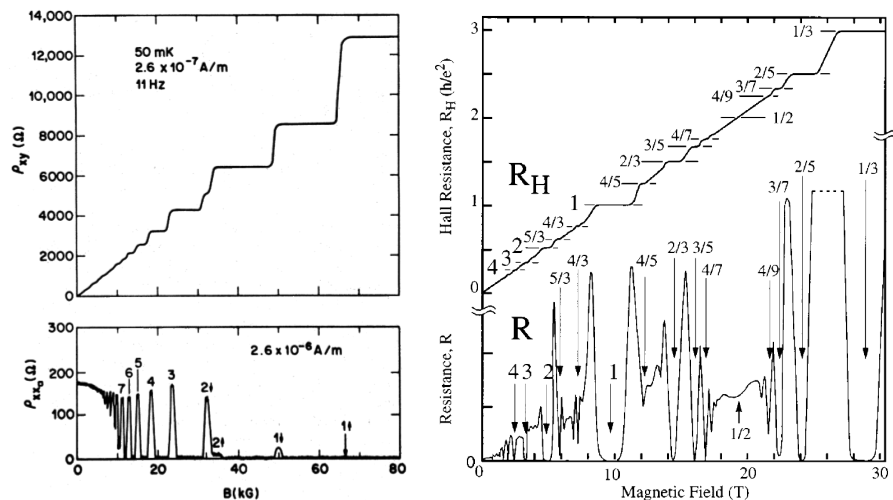


**Figure 1.1:** Diagonal and Hall resistance as a function of  $B$  in the IQHE (left) and in the FQHE (right). Note how the diagonal resistivity tends to vanish at the beginning of every plateau. The minima in the diagonal resistance constitute a much easier mean to detect fractions. Sources: [8][9]

The first account of these effects was given by Von Klitzing's study [10] in 1980 of the Hall effect in a MOSFET (metal-oxide-semiconductor field-effect transistor). His experimental setup operated at a temperature  $T = 1.5\text{K}$  and used a fixed magnetic field of  $B = 18\text{T}$ , corresponding to a magnetic length  $\ell \sim 104\mu\text{m}$ . The results indicated a quantization of the Hall resistance as a function of the density of electrons:

$$R_H = \frac{h}{ne^2} \quad (1.1.4)$$

where  $n$  is an integer. Other experiments with Si MOS systems [11] and GaAs-AlGaAs heterojunctions [8] put in light how this phenomenon is universal, in the sense that it presents itself in the exact same way in all known experimental setups: in particular the quantity  $h/e^2$  appears to be a universal constant. This is the Integral Quantum Hall Effect (IQHE).

The physics of the IQHE can be accounted for by an independent electrons theory. The key elements in the explanation lie in the presence of disorder in the sample and in the energy quantization of the electrons.

As the experimental techniques were perfected some unexpected plateaux

## 1.2. LANDAU LEVELS

in the Hall resistance were observed at fractional multiples of  $h/e^2$ :

$$R_H = \frac{h}{fe^2} \quad (1.1.5)$$

with  $f = 1/3$  was observed for the first time in 1982 by Tsui, Stormer and Gossard [1] in GaAs heterostructures and started the study of the fractional effect (FQHE). Their discovery was made possible by the very low working temperature they reached (50 mK), two orders of magnitude smaller than that employed by Von Klitzing. In their setup they had a particle density of about  $4.0 \cdot 10^{15} \text{m}^{-2}$  and a magnetic field of less than 8T, corresponding to a magnetic length  $\ell \sim 157 \mu\text{m}$ .

In the absence of magnetic field, an electron gas in its ground state is observed to form a Wigner crystal which minimizes the electrostatic repulsion. Note that in QHE experiments, the magnetic length, which quantifies the spacial extension of the electronic wavefunctions, is much larger than the typical Wigner lattice constant, which in 2D is  $\sim 1.6 \text{nm}$  [12]. This is a symptom that in the context of the quantum Hall problem, the host lattice does not play a relevant role, as the wavefunctions extend over so many lattice sites.

After the discovery of the first fractional plateau (which granted Laughlin, Tsui and Stormer a shared Nobel prize in 1998), plateaux at more than other 50 fractions were observed such as those in references [13][14].

Experimentally, crucial elements that made these discoveries possible were the possibility to reach lower temperatures, stronger magnetic fields and availability of much purer samples.

Unlike the integer effect, the FQHE cannot be explained neglecting the interactions between electrons: here the coulombic repulsion plays a fundamental role. A successful theory for the fractional effect explains it as the integer effect for topological particles called composite fermions (CF) [6].

## 1.2 Landau levels

The theoretical explanations for the integral and fractional effects are quite different but both involve a quantum mechanical treatment of the motion of electrons in a magnetic field.

### 1.2.1 Energy spectrum

We start off by studying the single electron in a magnetic field. The single particle hamiltonian is

$$\mathcal{H} = \frac{1}{2m_e} \left( \mathbf{p} + \frac{e}{c} \mathbf{A} \right)^2 \quad (1.2.1)$$

## 1. UNCORRELATED ELECTRONS IN UNIFORM MAGNETIC FIELD

where  $\mathbf{A} = \mathbf{A}(\mathbf{x})$  is the vector potential. Let us define a dynamical momentum

$$\boldsymbol{\pi} := \mathbf{p} + \frac{e}{c} \mathbf{A} \quad (1.2.2)$$

and rewrite the hamiltonian as

$$\mathcal{H} = \frac{1}{2m_e} \boldsymbol{\pi}^2 \quad (1.2.3)$$

We observe that the components of  $\boldsymbol{\pi}$  do not commute with each other. Instead, using the coordinate representation promptly shows that

$$[\pi_1, \pi_2] = -i\hbar \frac{eB}{c} \mathbb{1} = -i \frac{\hbar^2}{\ell^2} \mathbb{1} \quad (1.2.4)$$

From now we will be using units where the magnetic length  $\sqrt{\hbar c/eB} =: \ell \equiv 1$ . Since the commutator (1.2.4) is proportional to the identity, the hamiltonian of our problem is unitarily equivalent to that of an harmonic oscillator. Hence we expect an energy spectrum of the form  $\epsilon_n \propto (n + 1/2)$ ,  $n = 0, 1, 2, \dots$ . Thus we define a pair of ladder operators

$$a := \frac{\pi_1 - i\pi_2}{\hbar\sqrt{2}} \quad a^\dagger := \frac{\pi_1 + i\pi_2}{\hbar\sqrt{2}} \quad (1.2.5)$$

so that their commutator is  $[a, a^\dagger] = \mathbb{1}$ . This way the hamiltonian (1.2.3) can be rewritten as a function of the number operator  $a^\dagger a$  and we find the energy spectrum in the expected form:

$$\epsilon_n = \hbar\omega_c \left( n + \frac{1}{2} \right) \quad (1.2.6)$$

where the cyclotron frequency is defined by  $\omega_c := eB/m_e$ . These energy levels are named Landau levels after L.D. Landau who solved the problem [15] when quantum mechanics was a very recent invention.

In passing, note that the energy separation between adjacent Landau levels  $\hbar\omega_c$  increases linearly with the magnetic field strength.

### 1.2.2 Degeneracy

In the classical analogue of this problem, solving the equation of motion gives the solution

$$\begin{pmatrix} x(t) \\ y(t) \end{pmatrix} = \begin{pmatrix} X_0 \\ Y_0 \end{pmatrix} + r \begin{pmatrix} \cos(\omega_c t) \\ \sin(\omega_c t) \end{pmatrix} \quad (1.2.7)$$

i.e. a circular uniform orbit of radius  $r > 0$  around the center  $(X_0, Y_0)$ . Using the expressions for the velocities shows that

$$\begin{pmatrix} X_0 \\ Y_0 \end{pmatrix} = \begin{pmatrix} x + \dot{y}/\omega_c \\ y - \dot{x}/\omega_c \end{pmatrix} \quad (1.2.8)$$

## 1.2. LANDAU LEVELS

These classical results will help us in determining the degeneracy of the Landau levels in the quantum mechanical context. Following [16] we define by analogy the following quantum mechanical orbit center operators

$$X_0 := x + \frac{1}{\omega_c} \frac{dy}{dt} = x - \frac{\pi_2}{m_e \omega_c} \quad Y_0 := y - \frac{1}{\omega_c} \frac{dx}{dt} = y + \frac{\pi_1}{m_e \omega_c} \quad (1.2.9)$$

as well as a corresponding quantum orbit radius operator  $R_0^2 = X_0^2 + Y_0^2$ . The time derivatives are computed using Heisenberg's equation. Direct calculation shows that  $[\mathcal{H}, X_0] = [\mathcal{H}, Y_0] = 0$ , while  $[X_0, Y_0] = i\hbar/m_e\omega_c$ , which implies that the Landau levels are certainly degenerate.

We will now show that this degeneracy is due to angular momentum. To do this, let us fix the symmetric gauge for the vector potential, so that

$$\mathbf{A}(\mathbf{x}) = \frac{1}{2} \mathbf{B} \times \mathbf{x} = \frac{B}{2} (-y, x) \quad (1.2.10)$$

Then the angular momentum in this 2-D problem is given by

$$L \equiv L_3 = xp_y - yp_x = \frac{eB}{2c} (r_c^2 - R_0^2) \quad (1.2.11)$$

where  $r_c^2 := (x - X_0)^2 + (y - Y_0)^2$ . Now, the angular momentum is indeed a constant of motion, since  $[\mathcal{H}, L] = 0$ . But the physical meaning of  $L$  in the presence of an external magnetic field can be very unusual: in this context it quantifies the radial position of the orbit center.

Let us write the angular momentum spectrum as  $L = -\hbar m$ ,  $m \in \mathbb{Z}$ . Next, the hamiltonian (1.2.3) can be written in terms of  $r_c$  as  $\mathcal{H} = \frac{1}{2} m_e \omega_c^2 r_c^2$ , so the spectrum of the  $r_c^2$  operator is found to be:

$$r_c^2 = \frac{2\hbar}{m_e \omega_c} \left( n + \frac{1}{2} \right) \quad (1.2.12)$$

Now, the operator  $R_0^2 = X_0^2 + Y_0^2$  is again unitarily equivalent to an harmonic oscillator hamiltonian. From this observation it follows that its spectrum is  $R_0^2 = 2(m' + 1/2)$ , with  $m' = 0, 1, 2, \dots$ . Substituting back in (1.2.11) the spectra of operators  $L, r_c^2, R_0^2$  gives the relation:

$$m = m' - n \quad (1.2.13)$$

Thus, for a fixed energy,  $L$  is unbounded in one direction and bounded in the other. A real physical system usually has a finite size. Since the orbit center must lie inside the system, this puts an upper bound on  $R_0^2$ , which in turn implies that there must be a maximum admitted value for  $m'$ . Thus in real systems  $L$  is bounded in both directions and  $m = -n, -n+1, \dots, -n+m'_{\max}$ .

We are now ready to quantify the degeneracy of the Landau levels. Consider a disk shaped system of surface  $S$ . In units of  $\ell$ , the  $R_0^2$ -quantum is

## 1. UNCORRELATED ELECTRONS IN UNIFORM MAGNETIC FIELD

simply 2, to which is naturally associated a surface quantum  $2\pi$ . Hence  $S/2\pi$  is the degeneracy of each Landau level and  $G := 1/2\pi$  is the corresponding degeneracy per unit area. If  $\rho_0$  is the number density of electrons on the surface, we define the filling factor

$$\nu := \frac{\rho_0}{G} = 2\pi\rho_0 \quad (1.2.14)$$

which represents the number of filled Landau levels.

Let us now define a couple of ladder operators for  $R_0^2$  (or equivalently for the angular momentum):

$$b := \frac{X_0 + iY_0}{\sqrt{2}} \quad b^\dagger := \frac{X_0 - iY_0}{\sqrt{2}} \quad (1.2.15)$$

which verify  $[b, b^\dagger] = \mathbb{1}$ . From direct calculation we find that the ladder operators for  $R_0^2$  commute with those for the energy levels.

Diagonalizing together the complete set of commuting operators  $\{\mathcal{H}, L\}$  we can express a basis for the state space as

$$|n, m\rangle = \frac{(b^\dagger)^{m+n}}{\sqrt{(m+n)!}} \frac{(a^\dagger)^n}{\sqrt{n!}} |0, 0\rangle \quad (1.2.16)$$

Our next objective is finding the eigenfunctions for the single electron problem. To do so we will work in particular holomorphic function spaces that will make our calculations swifter.

### 1.2.3 Bargmann space

The commutation relations between position and momentum operators are central to quantum mechanics. Defining a family of ladder operators  $\{a_i\}$  on a Hilbert space permits to find the equivalent relations  $[a_i, a_j^\dagger] = \delta_{ij}\mathbb{1}$  known as canonical commutation relations (CCR).

Consider the space  $H(\mathbb{C}^d)$  of holomorphic functions  $F : \mathbb{C}^d \rightarrow \mathbb{C}$  and define the operators of multiplication and derivation. Then their commutator is computed to be

$$\left[ \frac{\partial}{\partial z_i}, z_j \right] = \delta_{ij}\mathbb{1} \quad (1.2.17)$$

i.e. they match the CCR. Unlike ladder operators, multiplication and derivation operators are not adjoints of one another in a function space with the usual inner product. Nonetheless it is possible to define an inner product so that  $(\frac{\partial}{\partial z_j})^\dagger = z_j$ ; indeed Bargmann in [17] found a Hilbert space in which these operators would be adjoints of one another.

## 1.2. LANDAU LEVELS

**Definition 1.2.1** (Bargmann space). Let  $HL^2(\mathbb{C}^d, \mu)$  be the space of holomorphic functions

$$HL^2(\mathbb{C}^d, \mu) := \left\{ F \in H(\mathbb{C}^d) : \int_{\mathbb{C}^d} d\mu |F(z_1, \dots, z_d)|^2 < \infty \right\} \quad (1.2.18)$$

where

$$d\mu := (\pi\sqrt{2})^{-d} \exp \left[ -\frac{1}{2} \sum_{i=1}^d |z_i|^2 \right] d^d z \quad (1.2.19)$$

and  $d^d z$  is simply the Lebesgue measure on  $\mathbb{C}^d = \mathbb{R}^{2d}$ . Then  $HL^2(\mathbb{C}^d, \mu)$  is called Bargmann space.

Since it is a closed subspace of the Hilbert space  $L^2(\mathbb{C}^d, \mu)$  the Bargmann space is also an Hilbert space. An orthonormal basis for this space is given by the following set of functions

$$\left\{ \prod_{j=1}^d \frac{z^{n_j}}{\sqrt{2^{n_j+1/2} n_j!}} : (n_j) \subset \mathbb{N}^d \right\} \quad (1.2.20)$$

By construction, in Bargmann space derivation and multiplication operators are adjoints of one another and verify the CCR. Note that, since the inner product in this space is not the standard one, operators that have specific properties (e.g. are unitary, hermitian, etc.) in this space may not have them in function spaces with the standard inner product (and viceversa).

Following Hall [18] we now recall a theorem of central importance for quantum mechanics, because it helps to justify the choice of  $L^2$  as a Hilbert space and the coordinate representation for the position and momentum operators.

**Theorem 1.2.1** (Stone-von Neumann). *Let  $A_1, \dots, A_d$  and  $B_1, \dots, B_d$  be self-adjoint and possibly unbounded operators on a Hilbert space  $H$ . Suppose the following conditions hold:*

1. (CCR) For  $j, k = 1, \dots, d$  and for  $r, s \in \mathbb{R}$  we have

$$\begin{aligned} \left[ e^{irA_j}, e^{isA_k} \right] &= 0 \\ \left[ e^{irB_j}, e^{isB_k} \right] &= 0 \\ e^{irA_j} e^{isB_k} &= e^{-irs\delta_{jk}} e^{isB_k} e^{irA_j} \end{aligned}$$

2. (Irreducibility) If  $V \subset H$  is a closed subspace of  $H$  invariant under  $e^{irA_j}$  and  $e^{isB_k}$  for all  $j, k$  and all  $r, s$ , then either  $V = \{0\}$  or  $V = H$ .

## 1. UNCORRELATED ELECTRONS IN UNIFORM MAGNETIC FIELD

Then there is a unitary map  $U : H \rightarrow L^2(\mathbb{R}^d, dx)$  such that  $U e^{irA_j} U^\dagger = e^{irQ_j}$  and  $U e^{isB_k} U^\dagger = e^{isP_k}$  are the canonical position and momentum operators exponentiated.

We have formulated the theorem using operators in their exponentiated form: this makes them bounded, which avoids domain problems. For the sake of clarity we note how this result holds not only for position and momenta operators but also for any other operators satisfying the same conditions.

This theorem is central in validating the use of unconventional representations in quantum mechanics: it affirms that if we have a Hilbert space and in it are defined operators that meet the hypotheses of the theorem, then these operators are merely different but equivalent ways to express the canonical position and momentum operators (or equivalently the ladder operators). Ultimately,  $L^2$  is not special in any way and its choice is a matter of convenience. Up to unitary equivalence, there is a unique irreducible representation of the CCR.

In the case of the Bargmann space, it can be shown that the Stone-von Neumann theorem holds. This implies we can represent creation and annihilation operators as multiplication and derivation operators on Bargmann space and there exists a unitary operator to map them to canonical ladder operators. This operator is the integral Bargmann transform

$$U : L^2(\mathbb{R}^d, dx) \rightarrow HL^2(\mathbb{C}^d, \mu) \quad (1.2.21)$$

$$U \left( \frac{Q_j + iP_j}{\hbar\sqrt{2}} \right) U^\dagger = \frac{\partial}{\partial z_j} \quad (1.2.22)$$

$$U \left( \frac{Q_j - iP_j}{\hbar\sqrt{2}} \right) U^\dagger = z_j \quad (1.2.23)$$

In the next section we will be able to appreciate the usefulness of this representation in making the calculations much swifter.

### 1.2.4 Eigenfunctions

We wish to find the common eigenfunctions of  $\mathcal{H}, L$  in Bargmann space. To do this, we represent both sets of ladder operators as multiplication and derivation operators on Bargmann space functions:

$$\begin{cases} a^\dagger & \mapsto \frac{w}{\sqrt{2}} \\ a & \mapsto \sqrt{2} \frac{\partial}{\partial w} \\ b^\dagger & \mapsto \frac{z}{\sqrt{2}} \\ b & \mapsto \sqrt{2} \frac{\partial}{\partial z} \end{cases} \quad (1.2.24)$$

## 1.2. LANDAU LEVELS

Expressing  $b^\dagger$  in terms of the spatial coordinates leads to the identification  $z = x - iy$  in units of  $\ell$ . The ground state is found by imposing  $a|0,0\rangle = b|0,0\rangle = 0$ , which implies  $\Psi_{00}(w, z) = 2^{-1/2}$ . All the other eigenfunctions are obtained from (1.2.16):

$$\Psi_{nm}(w, z) = \frac{z^{m+n}}{\sqrt{2^{m+n+1/2} (m+n)!}} \frac{w^n}{\sqrt{2^{n+1/2} n!}} \quad (1.2.25)$$

From now on we will only be interested to the lowest Landau level (LLL): so fixing  $n = 0$  and integrating out  $w$  gives

$$\Psi_m(z) = \frac{z^m}{\sqrt{2^{m+1/2} m!}} \quad (1.2.26)$$

In passing we emphasize how, by linearity, any polynomial in  $z$  is an eigenfunction of  $\mathcal{H}$  relative to the LLL.

It is useful to have a way to retrieve the eigenfunctions in  $L^2(\mathbb{R}^2)$ , more commonly used in the literature. Let  $\phi(z)$  be a almost-everywhere-nonzero function and write the identity

$$\int d\mu |\Psi_m(z)|^2 = \int \frac{dz}{\pi\sqrt{2}} e^{-|z|^2/2} |\Psi_m(z)|^2 \quad (1.2.27)$$

$$= \int \frac{dz}{\pi\sqrt{2}} \frac{e^{-|z|^2/2}}{|\phi(z)|^2} |\phi(z)\Psi_m(z)|^2 \quad (1.2.28)$$

Choosing

$$\phi(z) = \frac{e^{-|z|^2/4}}{\sqrt{\pi\sqrt{2}}} \quad (1.2.29)$$

we can build a norm-preserving map

$$A : HL^2(\mathbb{C}, \mu) \rightarrow L^2(\mathbb{R}^2) \quad (1.2.30)$$

$$\Psi_m \mapsto \phi\Psi_m =: \tilde{\Psi}_m \quad (1.2.31)$$

In this fashion we obtain the more familiar normalized eigenfunction

$$\tilde{\Psi}_m(z) = \frac{1}{\sqrt{2\pi 2^m m!}} z^m e^{-|z|^2/4} \quad (1.2.32)$$

where  $z = x - iy$ . Note that the obtained eigenfunctions are no longer holomorphic<sup>1</sup>, since they fail to satisfy Cauchy-Riemann equations.

---

<sup>1</sup>The term  $e^{-|z|^2/4}$  is itself not holomorphic and compromises the rest of the wavefunction.

### 1.3 Integer Quantum Hall Effect

Now we have all the elements to gain a basic understanding of the physics of the integer effect through a useful semiclassical argument. In real setups, the electrons feel not only the coulombic repulsion of one another (unessential to the IQHE) and the magnetic field: an impurity potential is also present. It generates a landscape of peaks and troughs, varying on a bigger length scale than that of the magnetic length in conditions of strong magnetic field. Hence the energy of an electron will be given by the sum of the hamiltonian (1.2.1) and the impurity term. This way the Landau levels are broadened and a distinction between localized and delocalized states comes to be. Electrons moving along equipotential lines of the impurity potential, which are closed, are in localized states.

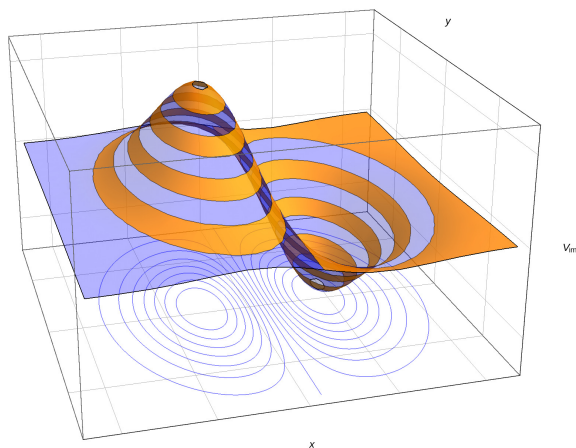


**Figure 1.2:** An example of impurity potential acting in the IQHE and a few equipotential lines.

The existence of localized states explains the presence of plateaux in  $R_H$ . First of all, note that from the point of view of quantum Hall effects, tuning the magnetic field and changing the electron density are equivalent operations. Now, starting from a filling factor  $\nu = n$  and adding electrons (or holes) would change the value of the resistance in an ideal system. Accounting for the effects of impurities is thus essential in explaining the phenomenon. If the Fermi energy lies amongst localized states, then the added particles go to occupy localized states and thus do not contribute to conduction. Hence in this case the value of  $R_H$  does not change.

This model gives some insight on the nature of the plateaux, but does not explain the universality of the  $h/e^2$  constant: for example we could suspect a result for the  $\nu = n$  case such as  $R_H = B/ec\rho_{\text{deloc}}$  where  $\rho_{\text{deloc}}$  is the density of electrons in the delocalized states. Since this density can be very small, the Hall resistance could be very large and there would be no

### *1.3. INTEGER QUANTUM HALL EFFECT*

reason for it to be quantized as in (1.1.4).

This problem was solved by Laughlin [19] who showed that, as long as the Fermi energy lied between the  $n$ -th and the  $(n + 1)$ -th Landau levels, the Hall resistance would retain the value (1.1.4).

This page intentionally left blank.

## Chapter 2

# Fractional quantum Hall effect

In this chapter we discuss the physics of the fractional effect. We start by defining the problem and analyzing the aspects that distinguish it from the integer effect. We begin to gain an understanding of the phenomenon by finding an exact solution to the problem involving two and three electrons. We then move to the analysis of the full problem in Fock space and discuss Laughlin's ansatz for the ground state wavefunction.

### 2.1 Conceptual framework

In depth analyses of the IQHE, both experimental and numerical, have shown that the integer effect cannot produce plateaux at fractional filling factors. This is because there is a unique delocalized state for each Landau level. For this reason a theoretical account of the fractional effect must provide a different explanation for the plateaux.

We can try and identify the responsible interaction by writing the full (first-quantized) Hamiltonian for a system of  $N$  electrons:

$$\mathcal{H} = \frac{1}{2m} \sum_{j=1}^N \left( \mathbf{p}_j + \frac{e}{c} \mathbf{A}_j \right)^2 + \sum_{j=1}^N \sum_{k < j}^N \frac{e^2/\varepsilon}{|\mathbf{x}_j - \mathbf{x}_k|} + g\mu_B \mathbf{B} \cdot \mathbf{S} + V_{\text{imp}} \quad (2.1.1)$$

From left to right these are respectively the kinetic term (accounting also for the interaction with the magnetic field), the coulombic repulsion term, the Zeeman splitting term and finally the impurity potential of the sample. Momentarily setting  $c = 1$  and using values for the parameters typical of GaAs-AlGaAs heterojunctions, we can compare the relative importance of the various terms:

$$\ell = \sqrt{\frac{\hbar c}{eB}} \approx \frac{25}{\sqrt{B}} \text{nm} \quad \hbar\omega_c = \hbar \frac{eB}{mc} \approx 20k_B B \text{ J} \quad (2.1.2)$$

## 2. FRACTIONAL QUANTUM HALL EFFECT

where the magnetic field strength  $B$  is to be expressed in Tesla and the mass  $m = 0.067m_e$  is the band mass in the sample. Using  $\varepsilon = 12.6$  and Landé factor  $g = -0.44$  we quantify the Coulomb and Zeeman energies roughly as

$$E_{\text{Coulomb}}(B) = \frac{e^2}{\varepsilon\ell} \approx 50k_B\sqrt{B} \text{ J} \quad (2.1.3)$$

$$E_{\text{Zeeman}}(B) = g\mu_B B = \frac{1}{2} \frac{m_b}{m_e} \hbar\omega_c \approx 0.3k_B B \text{ J} \quad (2.1.4)$$

Comparing the characteristic energies of the different terms leads us to the following approximations:

- We *neglect the impurity potential*: although it is essential to the explanation of plateaux in the integer effect, no significant physics is lost by switching it off in this context. This is because disorder causes the plateaux but these can only appear if there are gaps in the state occupancy of electrons. These gaps thus logically precede the plateaux. A model for the quantum hall effect must then explain the gaps: since for the FQHE this can be done without accounting for impurities, they add nothing significant to the underlying physics of the phenomenon.
- We consider *fully polarized electrons*: i.e. the spin degree of freedom is frozen. If all spins are aligned, the Zeeman term in the hamiltonian is constant and can be dropped. This approximation is not necessarily appropriate for all experimental realizations. Anyways, in strong magnetic fields,  $E_{\text{Coulomb}}/E_{\text{Zeeman}} \rightarrow 0$  which implies that electrostatic repulsion energy is not enough to flip a spin.
- We *consider the  $B \rightarrow \infty$  limit*, at fixed filling factor, which agrees well with the previous approximation. Since  $E_{\text{Coulomb}}/\hbar\omega_c \rightarrow 0$  this justifies neglecting LL mixing caused by electrostatic repulsion (which is the only interaction we haven't neglected). Keeping the fixed filling factor constant is crucial in performing this limit, otherwise the limit would imply  $\nu \rightarrow 0$ . To avoid this we must also have the electron number density  $\rho_0 \rightarrow 0$ .

It is vital that the second hypothesis is applied: this is because  $E_{\text{Zeeman}}/\hbar\omega_c$  is not necessarily small in strong magnetic field. So, even in the limit  $B \rightarrow \infty$  there could in principle be LL mixing caused by spin-orbit interaction, even though energetically very unfavorable. If we freeze the spin degree of freedom before operating the limit this problem is avoided.

All of these approximations are introduced because they simplify the problem significantly, getting rid of aspects that are not fundamental and thus exposing only the essential physics of the FQHE.

## 2.2 Exact solution for the three particle problem

Following Laughlin in [2], in this section we find exact solutions for the problem of two and three interacting electrons, given the working hypotheses given above. Now, the problem of three particles interacting through a  $1/r$  potential usually does not have analytical solutions: the reason why in this context we can solve it rests in the projection on the LLL. A 2-body problem is an effective 1-body problem, since we can focus on the internal degree of freedom, discarding the trivial center of mass degree of freedom. Projecting on the LLL turns the problem in an effective 0-body problem, since it takes away another degree of freedom. The same reasoning applied to the 3-body problem reduces it to an effective 1-body problem, which is thus solvable.

### 2.2.1 Two interacting particles

We start by choosing a coordinate representation in which for  $j = 1, 2$  the position of each electron is specified by the complex number  $z_j = x_j - iy_j$  and writing the two particle hamiltonian in it:

$$\mathcal{H} = \frac{1}{2m_e} \left( -i\hbar\nabla_1 + \frac{e}{c}\mathbf{A}(z_1) \right)^2 + \frac{1}{2m_e} \left( -i\hbar\nabla_2 + \frac{e}{c}\mathbf{A}(z_2) \right)^2 + \frac{e^2}{|z_1 - z_2|} \quad (2.2.1)$$

where  $\nabla_j = (\partial_{x_j}, \partial_{y_j})$ . We have taken  $\varepsilon = 1$  for convenience. Next, we choose the symmetric gauge for the vector potential, so that its expression is the same as in (1.2.10). We can separate the center of mass from the internal degree of freedom by performing the change of variables<sup>1</sup>:

$$\begin{cases} \bar{z} & := \frac{z_1 + z_2}{2} \\ z_a & := \frac{z_1 - z_2}{\sqrt{2}} \end{cases} \quad \begin{cases} \bar{\mathbf{p}} & := \mathbf{p}_1 + \mathbf{p}_2 \\ \mathbf{p}_a & := \frac{\mathbf{p}_1 - \mathbf{p}_2}{\sqrt{2}} \end{cases} \quad (2.2.2)$$

where  $\mathbf{p}_a$  has components  $p_{x_a}$  and  $p_{y_a}$ . Conjugate variables for the  $z_a$  degree of freedom are respectively  $x_a, p_{x_a}$  and  $y_a, p_{y_a}$ :

$$[x_a, p_{x_a}] = i\hbar\mathbb{1} \quad [y_a, p_{y_a}] = i\hbar\mathbb{1} \quad (2.2.3)$$

Similar relations hold for the center of mass degree of freedom. The vector potential transforms as

$$\mathbf{A}(\bar{z}) = \frac{\mathbf{A}(z_1) + \mathbf{A}(z_2)}{2} \quad \mathbf{A}(z_a) = \frac{\mathbf{A}(z_1) - \mathbf{A}(z_2)}{\sqrt{2}} \quad (2.2.4)$$

The kinetic part of the hamiltonian (2.2.1) rewritten in the new variables is

$$\mathcal{H}_{\text{kin}} = \frac{1}{2m} \left( \frac{1}{\sqrt{2}}\bar{\mathbf{p}}_a + \frac{e\sqrt{2}}{c}\mathbf{A}(\bar{z}) \right)^2 + \frac{1}{2m} \left( \mathbf{p}_a + \frac{e}{c}\mathbf{A}(z_a) \right)^2 \quad (2.2.5)$$

---

<sup>1</sup>Notice how the transformation has a Jacobian different from 1.

## 2. FRACTIONAL QUANTUM HALL EFFECT

The two terms are mutually commuting. Since the potential will not contain any terms from the center of mass degree of freedom, we discard the first term, whose eigenfunctions and eigenvalues we already know from Chapter 1. Focusing on the internal degree of freedom, the relevant hamiltonian becomes:

$$\mathcal{H}_{\text{int}} = \frac{1}{2\mu} \left( -i\hbar\nabla_a + \frac{e}{c}\mathbf{A}(z_a) \right)^2 + \frac{e^2}{\sqrt{2}|z_a|} \quad (2.2.6)$$

where  $\nabla_a = (\partial_{x_a}, \partial_{y_a}) = 2^{-1/2}(\partial_{x_1} - \partial_{x_2}, \partial_{y_1} - \partial_{y_2})$  and  $\mu = m_e$  is the reduced mass. The choice of the symmetric gauge for the vector potential causes  $\nabla \cdot \mathbf{A}$  to vanish. Hence, in the expansion of the kinetic term of the hamiltonian we have:

$$\mathcal{H}_{\text{kin}} = \frac{1}{2\mu} \left( -i\hbar\nabla_a + \frac{e}{c}\mathbf{A}(z_a) \right)^2 \quad (2.2.7)$$

$$= \frac{1}{2\mu} \left\{ -\hbar^2\Delta_a + \left(\frac{e}{c}\right)^2 \mathbf{A}^2(z_a) - \cancel{\frac{i\hbar e}{c}\nabla_a \cdot \mathbf{A}(z_a)} - \frac{i\hbar e}{c}\mathbf{A}(z_a) \cdot \nabla_a \right\} \quad (2.2.8)$$

$$= \frac{1}{2\mu} \left\{ -\hbar^2\Delta_a + \frac{e^2 B^2}{8c^2}|z_a|^2 + \frac{i\hbar e B}{4c}\partial_\phi \right\} \quad (2.2.9)$$

From this we deduce that the Schrödinger equation can be solved by separation of the variables:

$$\Psi(z_a) = \Psi(r, \phi) = R(r)\Phi(\phi) \quad (2.2.10)$$

with  $r := |z_a|$  and  $\phi := \text{Arg } z_a$ . The two-dimensional laplacian operator in polar coordinates is given by

$$\Delta_a = \partial_r^2 + \frac{1}{r}\partial_r + \frac{1}{r^2}\partial_\phi^2 \quad (2.2.11)$$

Next we observe that the hamiltonian (2.2.6) conserves the angular momentum  $L \equiv L_3 = x_a p_{y_a} - y_a p_{x_a} = -i\hbar\partial_\phi$ . Substituting (2.2.9), (2.2.11) and the angular momentum spectrum  $L = \hbar m$ ,  $m = 0, 1, 2, \dots$  in (2.2.6) we find the equation for the radial part of the eigenfunction  $R = R(r)$ :

$$-\frac{\hbar^2}{2\mu} \left( \frac{d^2 R}{dr^2} + \frac{1}{r} \frac{dR}{dr} - \frac{m^2}{r^2} R \right) + \frac{1}{2}\mu\omega_c^2 r^2 R(r) - \frac{1}{2}\hbar\omega_c m R(r) + \frac{e^2}{\sqrt{2}r} R(r) = \epsilon R(r) \quad (2.2.12)$$

which is just the radial Schrödinger equation for a two dimensional harmonic oscillator, with an added potential term  $V' = e^2/\sqrt{2}r$ . The angular part of the wavefunction is found to be

$$\Phi(\phi) = e^{-im\phi} \quad (2.2.13)$$

## 2.2. EXACT SOLUTION FOR THE THREE PARTICLE PROBLEM

The potential term  $V'$  constitutes a repulsive core caused by the coulombic repulsion between electrons. Treating it as small leads to an evaluation of the energy eigenvalue in a first order perturbative approximation. Remembering that we are restricting the analysis to the LLL we have

$$\epsilon_m = \epsilon_{LLL} + \langle m|V'|m\rangle = \frac{1}{2}\hbar\omega_c + \langle m|V'|m\rangle \quad (2.2.14)$$

where the states  $|m\rangle$  are the eigenstates of the unperturbed hamiltonian. Since letting  $V' = 0$  in (2.2.6) leads to the hamiltonian (1.2.1), these states are represented by the functions (1.2.32).

The expected value of the perturbation can be computed through the following calculation

$$\left\langle m \left| \frac{1}{r} \right| m \right\rangle = \int_{\mathbb{C}} dz \Psi^*(z) \frac{1}{|z|} \Psi(z) \quad (2.2.15)$$

$$= \frac{1}{2^{m+1}\pi m!} \int_{\mathbb{C}} dz |z|^{2m-1} e^{-|z|^2/2} \quad (2.2.16)$$

$$= \frac{1}{2^m m!} \int_0^\infty dr r^{2m} e^{-r^2/2} \quad (2.2.17)$$

$$= \frac{\sqrt{2\pi}}{2^{m+1}} \frac{(2m-1)!!}{m!} = \sqrt{2\pi} \frac{(2m)!}{2^{2m+1}(m!)^2} \quad (2.2.18)$$

where the last line is an identity, easily provable by induction.

Computing the quantity  $\langle m|r^2|m\rangle = 2(m+1)$  over the unperturbed states gives us an intuitive interpretation for this model: as long as the coulombic interaction is small enough the two electrons orbit around their common center of mass, while the repulsion contributes a negative binding energy term. Numerical simulations show that the accuracy of the model increases with  $m$  and under usual experimental conditions it brings satisfactory results. This makes sense, since the electrostatic interaction expectation value (2.2.18) decreases with  $1/\sqrt{m}$  as  $m$  gets large, thus becoming more and more negligible.

### 2.2.2 Three interacting particles

As we anticipated in presenting this section, projection on the LLL and focusing on internal degrees of freedom make the three-body problem an effective one-body problem, turning it into solvable. The full hamiltonian is

## 2. FRACTIONAL QUANTUM HALL EFFECT

given by

$$\begin{aligned} \mathcal{H} = \frac{1}{2m_e} & \left\{ \left( -i\hbar\nabla_1 + \frac{e}{c}\mathbf{A}(z_1) \right)^2 + \left( -i\hbar\nabla_2 + \frac{e}{c}\mathbf{A}(z_2) \right)^2 \right. \\ & \left. + \left( -i\hbar\nabla_3 + \frac{e}{c}\mathbf{A}(z_3) \right)^2 \right\} + \frac{e^2}{|z_1 - z_2|} + \frac{e^2}{|z_2 - z_3|} + \frac{e^2}{|z_1 - z_3|} \end{aligned} \quad (2.2.19)$$

As before, we perform a coordinate change to isolate the center of mass degree of freedom

$$\begin{cases} \bar{z} & := \frac{z_1 + z_2 + z_3}{3} \\ z_a & := \sqrt{\frac{2}{3}} \left( \frac{z_1 + z_2}{2} - z_3 \right) \\ z_b & := \frac{z_1 - z_2}{\sqrt{2}} \end{cases} \quad \begin{cases} \bar{\mathbf{p}} & := \mathbf{p}_1 + \mathbf{p}_2 + \mathbf{p}_3 \\ \mathbf{p}_a & := \sqrt{\frac{2}{3}} \left( \frac{\mathbf{p}_1 + \mathbf{p}_2}{2} - \mathbf{p}_3 \right) \\ \mathbf{p}_b & := \frac{\mathbf{p}_1 - \mathbf{p}_2}{\sqrt{2}} \end{cases} \quad (2.2.20)$$

Rewriting (2.2.19) in the new variables and dropping the trivial dependence from the center of mass we obtain the hamiltonian for the internal degrees of freedom  $a, b$ :

$$\begin{aligned} \mathcal{H}_{\text{int}} &= \frac{1}{2\mu} \left\{ \left( -i\hbar\nabla_a + \frac{e}{c}\mathbf{A}(z_a) \right)^2 + \left( -i\hbar\nabla_b + \frac{e}{c}\mathbf{A}(z_b) \right)^2 \right\} + V' \\ V' &:= \frac{e^2}{\sqrt{2}} \left( \frac{1}{|z_b|} + \frac{1}{\left| \frac{\sqrt{3}}{2}z_a + \frac{1}{2}z_b \right|} + \frac{1}{\left| \frac{\sqrt{3}}{2}z_a - \frac{1}{2}z_b \right|} \right) \end{aligned} \quad (2.2.21)$$

Again we want to solve the problem considering the interaction  $V'$  as a small perturbation. We already know how the solution to the Schrödinger equation for uncorrelated particles is given in Bargmann space by the functions:

$$\varphi_{mn}(z_a, z_b) = \frac{1}{\sqrt{2^{m+n+1}m!n!}} z_a^m z_b^n \quad (2.2.22)$$

But, even though we are looking for the unperturbed eigenstates (i.e. with coulombic interaction switched off), we still need to account for Pauli's principle: namely our eigenfunctions must be antisymmetric under permutations of any two particles. Thus the functions (2.2.22) are not appropriate for this task. Still, they generate the whole state space, thus particular linear combinations of them will constitute a basis for the (smaller) space of admissible wavefunctions.

To find these combinations, we observe that for three particles and with the variables we defined, even permutations are precisely equivalent to a rotation of  $\pm 2\pi/3$  in the  $a, b$  space. Also, odd permutations are simply the

## 2.2. EXACT SOLUTION FOR THE THREE PARTICLE PROBLEM

parity transformation relative to  $z_b$ . Hence a convenient way to comply with Pauli's principle will be to require symmetry under rotations of  $\pm 2\pi/3$  and antisymmetry under  $z_b \mapsto -z_b$ . A way to satisfy these requirements is more easily achievable performing another change of variables:

$$\begin{cases} z_+ & := \frac{z_a + iz_b}{\sqrt{2}} \\ z_- & := \frac{z_a - iz_b}{\sqrt{2}} \end{cases} \quad (2.2.23)$$

Now, the transformation  $z_b \mapsto -z_b$  acts on the new variables as  $z_+ \leftrightarrow z_-$ . Also, rotations by an angle  $\theta$  in the  $a, b$  plane act as

$$\begin{cases} z_+ & \mapsto z_+ e^{i\theta} \\ z_- & \mapsto z_- e^{-i\theta} \end{cases} \quad (2.2.24)$$

Hence, all terms of the form  $(z_+ z_-)^k$  will be invariant under rotations by any  $\theta$  (but symmetric under odd permutations) for any integer  $k$ . Similarly all terms of the form  $z_+^k - z_-^k$  are antisymmetric under odd permutations: but from (2.2.24) we see that they are only symmetric under rotations by  $\theta = \pm 2\pi/3$  if  $k$  is a multiple of 3. All this motivates us to write the ansatz

$$\varphi_{mn}(z_+, z_-) = (z_+^{3m} - z_-^{3m})(z_+ z_-)^n \quad (2.2.25)$$

$$= z_+^{3m+n} z_-^n - z_+^n z_-^{3m+n} \quad (2.2.26)$$

We observe that the hamiltonian (2.2.21) commutes with the total angular momentum  $J = L_a + L_b$ . An argument in favour of the goodness of our ansatz is that the functions (2.2.26) diagonalize both the internal hamiltonian and the total angular momentum. Specifically they are eigenfunctions of  $J$  with eigenvalue  $\hbar M = \hbar(3m + 2n)$ .

Normalizing and expressing everything back in the  $z_a, z_b$  variables we find:

$$\begin{aligned} \varphi_{mn}(z_a, z_b) &= \frac{1}{\sqrt{2}} \frac{1}{\sqrt{2^{6m+4n+1}(3m+n)!n!}} \\ &\cdot \left[ (z_a + iz_b)^{3m} - (z_a - iz_b)^{3m} \right] (z_a^2 + z_b^2)^n \end{aligned} \quad (2.2.27)$$

Bringing the eigenfunctions back from Bargmann space to physical space and dividing them by  $i$  so that the polynomial part has real coefficients we finally obtain the eigenfunctions for the unperturbed internal hamiltonian:

$$\begin{aligned} \Psi_{mn}(z_a, z_b) &= \frac{1}{\sqrt{2^{6m+4n+1}(3m+n)!n!\pi^2}} \\ &\cdot \frac{(z_a + iz_b)^{3m} - (z_a - iz_b)^{3m}}{2i} (z_a^2 + z_b^2)^n e^{-(|z_a|^2 + |z_b|^2)/4} \end{aligned} \quad (2.2.28)$$

## 2. FRACTIONAL QUANTUM HALL EFFECT

A few observations are due. First of all, even though  $[\mathcal{H}_{\text{int}}, J] = 0$ , the  $M$  quantum number is not sufficient to specify an eigenfunction. In fact, except for the first few values of  $M$  there is degeneracy, i.e. for each  $M$  there is more than one possible couple  $(m, n)$  such that  $M = 3m + 2n$ . Moreover  $m$  can never be zero, otherwise the wavefunction is not admissible. This implies that  $M \in \mathbb{N} \setminus \{0, 1, 2, 4\}$ .

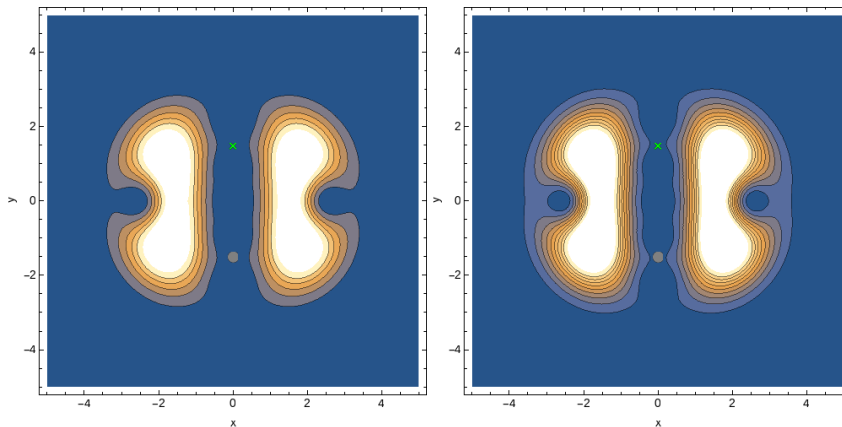


**Figure 2.1:** Comparison of the contour plots of charge densities for the states  $\Psi_{3,0}$  (left) and  $\Psi_{1,3}$  (right). The dot represents the center of mass and the cross represents one of the electrons. Both these points have been fixed to make the plot drawable. Note how the increase in the  $n$  quantum number causes the charge densities to shift towards the fixed electron and to be generally more spread.

We can now proceed in evaluating the effects of the coulombic interaction on the unperturbed eigenfunctions. To do this, we need to find the matrix elements of the electrostatic repulsion operator over the basis  $\{\Psi_{mn}\}$  of the admissible portion of state space i.e.

$$\left\langle m, n \left| \frac{1}{|z_b|} \right| m', n' \right\rangle \quad (2.2.29)$$

in units of  $3e^2/\ell\sqrt{2}$ . The factor 3 comes from the need to add contributions to the repulsion from all the three possible layouts of particles, differing from rotations of  $2\pi/3$  of the system. These matrix elements can only be nonzero if  $M = M'$ <sup>2</sup>, so from now we will only consider this case. To actually compute the matrix elements, consider a generic  $M$  and expand

---

<sup>2</sup>Since  $\left[ J, \frac{1}{|z_b|} \right] = 0$ , evaluation of  $\left\langle m, n \left| J \frac{1}{|z_b|} \right| m', n' \right\rangle$  gives the relation  $(M' - M) \left\langle m, n \left| \frac{1}{|z_b|} \right| m', n' \right\rangle = 0$ . Hence the matrix element can only be non-zero if  $M = M'$

## 2.2. EXACT SOLUTION FOR THE THREE PARTICLE PROBLEM

the polynomial part of the function (2.2.28):

$$\Psi_{mn}(z_a, z_b) = \frac{1}{\sqrt{2^{6m+4n+1}(3m+n)!n!\pi^2}} \sum_{k=1}^M c_k^{(m,n)} z_b^k z_a^{M-k} e^{-(|z_a|^2+|z_b|^2)/4} \quad (2.2.30)$$

where the  $c_k^{(m,n)}$  are real numbers. Then, neglecting all the normalization constants:

$$\left\langle m, n \left| \frac{1}{|z_b|} \right| m', n' \right\rangle \propto \quad (2.2.31)$$

$$\propto \sum_{k,l=1}^M \int_{\mathbb{C}^2} dz_a dz_b c_k^{*(m,n)} c_l^{(m',n')} \frac{1}{|z_b|} z_b^{*k} z_b^l z_a^{*M-k} z_a^{M-l} e^{-(|z_a|^2+|z_b|^2)/2} \quad (2.2.32)$$

$$\propto \sum_{k=1}^M c_k^{*(m,n)} c_k^{(m',n')} \left\langle k \left| \frac{1}{|z_b|} \right| k \right\rangle \quad (2.2.33)$$

Since the operator we are considering only depends from  $z_b$ , we have integrated in  $z_a$ . This resulted in a  $\delta_{kl}$  which turned the double sum into a single sum. Having done that, the remaining integral in  $z_b$  was simply the diagonal matrix element (2.2.18), which we have already calculated.

Substituting it in the previous expression and writing the normalization constant gives the final expression for the matrix element:

$$\left\langle m, n \left| \frac{1}{|z_b|} \right| m', n' \right\rangle = 2^{-M} \sqrt{\frac{2\pi}{(3m+n)!(3m'+n')!n!n'!}} \cdot \sum_{k=1}^M c_k^{*(m,n)} c_k^{(m',n')} \frac{(2k)!(M-k)!}{2^{2k} k!} \quad (2.2.34)$$

The matrices for the first few values of  $M$  have been calculated analytically and are found in Appendix A, together with their respective eigenvalues. The eigenvalues of the matrices indicate the shift in energy from the LLL caused by the presence of electrostatic repulsion.

By simple inspection, we see that degeneracy first appears for the value  $M = 9$ , which is three times the smallest possible value of angular momentum  $M = 3$ : hence this case corresponds to a filling factor of roughly  $1/3$ . Looking at the eigenvalues in cases where degeneracy is present we observe that the energy difference between states of adjacent  $M$  is usually considerably smaller than that between states with the same value of angular momentum. This observation is reasonable, if we consider Figure 2.1: increasing values of  $n$  get the electrons closer to each other, effectively increasing the overall energy by a tangible amount.

## 2. FRACTIONAL QUANTUM HALL EFFECT

Now, all of this may seem not significant for the problem of the FQHE, in which there is an extremely large number of electrons at play. To try and mimic that situation we can add a potential well to replicate the band energy. For convenience we choose it quadratic:

$$U = \frac{\alpha}{2}(|z_1|^2 + |z_2|^2 + |z_3|^2) = \frac{3}{2}\alpha|\bar{z}|^2 + \frac{\alpha}{2}(|z_a|^2 + |z_b|^2) \quad (2.2.35)$$

Hence, in addition to internal coulombic interaction  $V'$  we have to account also for  $U$ . Discarding the center of mass portion, we calculate (following the same logic as in (2.2.33)):

$$\begin{aligned} & \left\langle m, n \left| \frac{\alpha}{2} (|z_a|^2 + |z_b|^2) \right| m', n' \right\rangle \propto \\ & \propto \frac{\alpha}{2} \delta_{mm'} \delta_{nn'} \sum_{k=1}^M c_k^{*(m,n)} c_k^{(m',n')} \left( \langle k | |z_b|^2 | k \rangle + \langle M-k | |z_a|^2 | M-k \rangle \right) \end{aligned} \quad (2.2.36)$$

$$= \frac{\alpha}{2} \delta_{mm'} \delta_{nn'} \sum_{k=1}^M c_k^{*(m,n)} c_k^{(m',n')} [2(k+1) + 2(M-k+1)] \quad (2.2.37)$$

$$\propto \delta_{mm'} \delta_{nn'} \alpha (M+2) \quad (2.2.38)$$

This tells us that the presence of the potential well adds a contribution that makes states of lower total angular momentum energetically favorable.

The total potential to which the electrons are subject is thus  $V' + U$ . Hence the intensity of the potential well  $\alpha$  influences which  $\Psi_{mn}$  will be the true ground state. In particular, the ground state has an angular momentum  $M$  which is discontinuous as a function of  $\alpha$ : it assumes values that are integer multiples of 3. This is because  $M = 3m + 2n$  and for any  $\alpha$  the eigenstate minimizing the energy has  $n = 0$ .

Another relevant observable is the area enclosed by the triangle whose vertices are the three electrons. The corresponding operator can be written making use of Gauss's area formula: namely a triangle whose vertices are the points  $\{(x_i, y_i)\}_{i=1}^3$  has an area given by the determinant:

$$S = \frac{1}{2} \begin{vmatrix} 1 & 1 & 1 \\ x_1 & x_2 & x_3 \\ y_1 & y_2 & y_3 \end{vmatrix} \quad (2.2.39)$$

From this result we derive the operator associated to the area observable:

$$S = \frac{1}{2} \text{Im} [z_1^* z_2 + z_2^* z_3 + z_3^* z_1] \quad (2.2.40)$$

$$= \frac{\sqrt{3}}{4i} (z_a z_b^* - z_b z_a^*) \quad (2.2.41)$$

## 2.2. EXACT SOLUTION FOR THE THREE PARTICLE PROBLEM

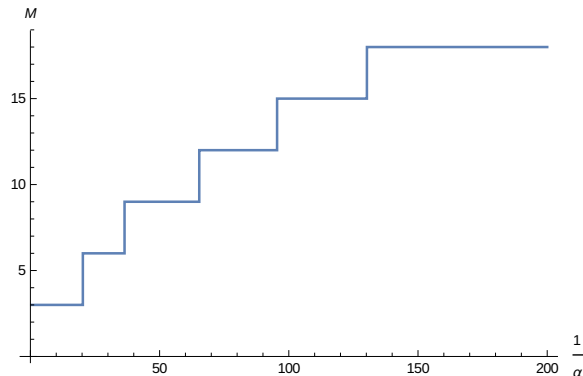


**Figure 2.2:** Total angular momentum  $M = 3m + 2n$  of the ground state as a function of inverse intensity of the potential well.  $M$  increases with jumps of 3 as  $\alpha$  decreases.  $\alpha$  is measured in units of  $\sqrt{3/2}e^2/\ell^3$ .

The relevant matrix element to be calculated is that of  $S^2$ , since  $\langle m, n|S|m', n'\rangle = 0$  for all  $(m, n), (m', n')$ . This is computed to be

$$\langle m, n|S^2|m', n'\rangle = \delta_{mm'}\delta_{nn'} \frac{3}{4} \left[ (3m)^2 + M + 2 \right] \quad (2.2.42)$$

So it depends linearly on  $M$ . Hence, also the rms of the area will depend discontinuously on  $\alpha$ , resembling the behaviour of the angular momentum in Figure 2.2. This means that making the potential well deeper does not get the particles closer to one another: this way the area is conserved on each plateau. Instead, when  $\alpha$  crosses a value corresponding to any plateau, the ground state changes and with it the configuration of the cluster, as well as the enclosed area. In other words, the cluster, when considered in any of the possible ground states, is incompressible.

This is an interesting property: in fact if it were found to hold also for the case of the many-body problem, then it might provide a basic explanation to the FQHE. In fact, adding electrons to the sample effectively deepens the band (i.e. increases  $\alpha$  in our model). If incompressibility held, then this operation would not cause excitations giving rise to plateaux in the conductivity, since the configuration of the particles would not change.

Sadly, this argument is a feeble one. This is because the many-body problem deals with a large, indeterminate number of interacting particles. Hence, the very meanings of configuration and incompressibility of cluster can be very different from those used in a two or three-body problem. For example, in the many-body problem, we can add particles to the system and keep using the same model; adding particles to a three-body problem forces us to change approach entirely.

All this considered, if incompressibility holds for the ground state of the many-body problem then it must be proved in a different way. Thus we must find a more suitable approach to explain the FQHE.

## 2.3 Many-body framework

As we said in the conclusion to the previous section, in treating the many-body problem we must be able to deal with an indeterminate number of particles. This is more easily done in the framework of second quantization, in which states are represented by vectors in Fock space:

$$\mathcal{F} := |0\rangle \oplus \mathcal{H}(1) \oplus \mathcal{H}(2) \oplus \dots \oplus \mathcal{H}(k) \oplus \dots \quad (2.3.1)$$

where  $|0\rangle$  is the vacuum state and  $\mathcal{H}(k)$  is the Hilbert space of  $k$  fermions.

### 2.3.1 The hamiltonian

To formulate the FQHE problem in this framework we first need to write the second-quantized hamiltonian operator. To achieve this, let  $N$  and  $m$  be the Landau level and the angular momentum quantum number respectively. We introduce the ladder operators  $a_{N,m}, a_{N,m}^\dagger$  which respectively destroy and create a particle in state  $|N, m\rangle$ . Now, all the approximations we mentioned in Section 2.1 remain valid. Thus the only remaining terms in the hamiltonian are the kinetic one and the coulomb interaction:

$$\hat{\mathcal{H}} = \sum_{(N,m)} \hbar\omega_c \left( N + \frac{1}{2} \right) \hat{a}_{N,m}^\dagger \hat{a}_{N,m} + \hat{\mathcal{H}}_{\text{coul}} \quad (2.3.2)$$

The sums are over the Landau level quantum number  $N \in \mathbb{N}$  and over the angular momentum quantum number  $m$ , which varies as discussed in Section 1.2.2. The interaction hamiltonian in Fock space can be obtained as a function of ladder operators

$$V = \frac{1}{2} \sum_{i \neq j} v(z_i, z_j) = \frac{1}{2} \sum_{i \neq j} \frac{e^2}{|z_i - z_j|} \quad (2.3.3)$$

The factor  $1/2$  is necessary to avoid double counting of interaction energies. Notice that the terms  $v(z_i, z_j)$  are naturally symmetric under exchange of particle labels. The image of the  $\hat{V}$  operator in Fock space is given by

$$\begin{aligned} \hat{\mathcal{H}}_{\text{coul}} = & \frac{1}{2} \sum_{(N_\alpha, m_\alpha)} \sum_{(N_\beta, m_\beta)} \sum_{(N_\gamma, m_\gamma)} \sum_{(N_\delta, m_\delta)} \hat{a}_{N_\alpha, m_\alpha}^\dagger \hat{a}_{N_\beta, m_\beta}^\dagger \hat{a}_{N_\delta, m_\delta} \hat{a}_{N_\gamma, m_\gamma} \\ & \cdot \langle N_\alpha, m_\alpha; N_\beta, m_\beta | v | N_\gamma, m_\gamma; N_\delta, m_\delta \rangle \end{aligned} \quad (2.3.4)$$

where we have used the condensed notation

$$|N_\alpha, m_\alpha; N_\beta, m_\beta\rangle \equiv |N_\alpha, m_\alpha\rangle \otimes |N_\beta, m_\beta\rangle$$

Now, the strong magnetic field approximation enables us to simplify the problem a lot more. Since it implies that LL mixing is negligible, there

### 2.3. MANY-BODY FRAMEWORK

cannot be jumps amongst energy levels. This means that the numbers of electrons in each LL are fixed.

Hence the kinetic term becomes an additive constant and can thus be dropped from the hamiltonian, together with all matrix elements containing Landau quantum numbers differing from  $N := \lfloor \nu \rfloor$  (floor function of the filling factor). The relevant hamiltonian then becomes:

$$\hat{\mathcal{H}} = \frac{1}{2} \sum_{m_\alpha} \sum_{m_\beta} \sum_{m_\gamma} \sum_{m_\delta} \hat{a}_{N,m_\alpha}^\dagger \hat{a}_{N,m_\beta}^\dagger \hat{a}_{N,m_\delta} \hat{a}_{N,m_\gamma} \langle N, m_\alpha; N, m_\beta | v | N, m_\gamma; N, m_\delta \rangle \quad (2.3.5)$$

In particular, since our analysis is limited to the LLL we fix  $N = 0$ . It is intended that the domain of this operator must be restricted to the portion of Fock space corresponding to the LLL. This is done formally through a projection. Nonetheless wrapping the operator inside projectors  $|LLL\rangle \langle LLL|$  introduces a complication. To avoid it we agree that the operator will act solely on LLL vectors. These approaches are operationally different, but overall equivalent, since by definition the action of an operator on a subspace of its domain is precisely the same as that of the same operator projected on that subspace. It is important to bear this argument in mind, otherwise the hamiltonian (2.3.5) would be effectively classical because it does not explicitly contain non-commuting operators.

A first look to the hamiltonian uncovers two peculiar features. The first one is the immense degree of correlation of the FQH system: if we quantify the strength of correlation in the system by the ratio of the interaction energy to the kinetic energy then we conclude that the system is completely correlated, because there is no kinetic term in the hamiltonian.

The other astonishing and worryingly fact is the total absence of any parameter depending upon the experimental realization of the system. In particular this means that a perturbative analysis is not possible, because there is no parameter on which to expand states and eigenvalues. There is no unperturbed state: if we set the interaction to zero we get an astronomical degeneracy of the ground state, even for unphysical systems with a few tens of electrons.

We are then left with the perspective that the only realistic path in solving the FQHE would be to tackle the full problem without any further help from approximations.

#### 2.3.2 Laughlin's ansatz

A breakthrough on this problem was operated by Laughlin in 1983: in his work [3] he found a tentative ground state wavefunction based on observation of fundamental features of the FQHE.

The reasoning behind Laughlin's ansatz can be schematized as follows:

- The wavefunction for a system of  $n_e$  electrons can be written as a

## 2. FRACTIONAL QUANTUM HALL EFFECT

linear combination of Slater determinants of the single particle wavefunctions, which we know to be (1.2.32). Thus its general form will be

$$\Psi_M(z_1, \dots, z_{n_e}) = f(z_1, \dots, z_{n_e}) \exp\left(-\sum_{j=1}^{n_e} |z_j|^2/4\right) \quad (2.3.6)$$

where  $f$  is a polynomial of the  $n_e$  complex representations of the positions of the electrons  $z_j = x_j - iy_j$ .

- As the hamiltonian conserves the total angular momentum we want the functions  $\Psi_M$  to be simultaneous eigenfunctions of  $J$  and  $\mathcal{H}$ . Now, every monomial of the polynomial, i.e.

$$\prod_j z_j^{m_j} \quad (2.3.7)$$

carries a total angular momentum  $\hbar M = \hbar \sum_j m_j$ . Since  $\Psi$  must be an eigenfunction of the total angular momentum, every monomial in  $f$  must carry the same  $M$ . In other words  $f$  must be an homogeneous polynomial in  $z_1, \dots, z_{n_e}$ .

- Since the exponential part of the eigenfunction is even under permutation of particle labels and the spin degree of freedom is frozen, to comply with Pauli's principle, the polynomial  $f$  must be completely antisymmetric.
- To make the shape of the polynomial more specific, we make use of physical intuition: since the interaction at play is a long range repulsion with a strong repulsive core, we expect that it will be less probable to find two electrons near one another. A way to translate this into an expression is to look for a polynomial of the form

$$f(z_1, \dots, z_{n_e}) = \prod_{j < k}^{n_e} g_{jk}(z_j - z_k) \quad (2.3.8)$$

where  $g_{jk}(z)$  is a polynomial in a single complex variable. In principle it could be different for any couple  $(j, k)$ . This type of wavefunction, known as Jastrow type, is very popular in the field of superconductivity, where it is employed in variational approaches. It is widely used to handle two-body correlations, but is not as effective with higher degrees of correlation.

- Combining the Jastrow type polynomial with the former conditions, the simplest function we can write is Laughlin's ansatz:

$$\Psi(z_1, \dots, z_{n_e}) = \prod_{j < k}^{n_e} (z_j - z_k)^q \exp\left(-\sum_{i=1}^{n_e} |z_i|^2/4\right) \quad (2.3.9)$$

### 2.3. MANY-BODY FRAMEWORK

$m$	$\langle \varphi_{3m}   \Psi_m \rangle$
1	1
3	0.99946
5	0.99468
7	0.99476
9	0.99573
11	0.99652
13	0.99708

**Table 2.1:** Overlaps of Laughlin’s wavefunction for three particles with the variational ground state wavefunctions studied in the three-body problem. The variational ground state wavefunctions for three interacting particles have an angular momentum quantum number of  $3m$ . Source [3].

with the restriction that  $q$  must be an odd integer to preserve antisymmetry. It is possible to show that rewriting the system’s hamiltonian, an analogy can be made with plasma systems. This method shows that the FQH filling factor is given in this case by  $\nu = 1/q$ . The extensive proof is given in [20].

Laughlin’s ansatz was written soon after the discovery of the  $1/3$  plateau, but it has proved to be very accurate for all filling factors of the form  $\nu = 1/q$  and their particle-hole symmetric  $\nu = 1 - 1/q$ . To quantify the accuracy of the ansatz we report in Table 2.1 the overlaps of Laughlin’s ansatz with the variational wavefunctions of the three-body problem. As we already said in the first chapter, there are many more fractions than those of Laughlin’s type ( $1/q$ ), that cannot be explained with Laughlin’s argument. So the problem cannot be said to be solved yet. Even more so, because there is no real justification at this level for why this ansatz manages to be so accurate.

Different explanations come from different models: in composite fermion theory a general solution is found, and Laughlin’s ansatz is recovered as a special case. Another approach was offered by complicated calculations by Haldane first in [21], then in [5] with Bernevig, where they found that the bosonic version of Laughlin’s wavefunctions can be mapped on a class of special functions known in mathematics as Jack symmetric functions.

In the next chapter we find quantitative results for the FQHE making use of the many-body approach presented in this section. This will be done by performing the analytical calculations of the coulomb matrix element in (2.3.5).

This page intentionally left blank.

## Chapter 3

# Coulomb interaction in the disk geometry

In this chapter we present the derivation of an analytic expression we obtained for the coulombic matrix elements in the disk geometry. The result is then employed to carry out the exact diagonalization of the hamiltonian in the LLL by means of a numerical analysis.

### 3.1 System geometry

Calculating the interaction matrix elements is usually of central importance for problems that can be treated perturbatively. Nonetheless, matrix elements have a fundamental role in the FQHE problem as well. This is clear when we consider that they effectively make up the many-body hamiltonian (2.3.5).

Since matrix elements are calculated amongst two vectors of a well defined basis of state space, they depend on the system setup. This is because the choice of a basis must be done in a smart way to reflect the symmetries and properties of the system, making the calculations as simple as possible. As in the hamiltonian there are no parameters depending on the experimental setup, the only way the wavefunctions can depend upon the system realization is through the geometry of the surface on which the 2D electrons move.

A choice that has become popular again in the last few years is that of a toroidal surface: this is obtained by taking a rectangular surface and applying periodic boundary conditions on both sides. In doing so, the effective topology obtained is that of a torus (the double periodicity amounts to going through the doughnut and all around it). This method avoids the problem of a confining potential, which gives rise to edge states. Of course a basis of eigenstates of the interaction-free hamiltonian in this geometry must be obtained specifically (a good way to start is adopting the Landau

### 3. COULOMB INTERACTION IN THE DISK GEOMETRY

gauge instead of the axial one).

The popularity of this geometry is due to the fact that, in the limit of a thin torus the ground state can be obtained exactly and it is found to be a Tao-Thouless (TT) state. Also, in the thin torus limit the matrix elements only depend on the reciprocal difference amongst angular momentum quantum numbers.

Another very pleasing fact about this geometry is that it is possible to map the quantum Hall problem onto a one dimensional lattice [22]. In particular, the ground state at filling factor  $\nu = p/q$  is a one dimensional crystal with  $p$  electrons in lattice sites of size  $q$ . Of course one drawback of the thin torus limit is that it is quite unphysical.

The spherical geometry was also studied extensively. In particular, Haldane in [23] introduced a translationally invariant version of Laughlin's state on a sphere. In the same work he found a hierarchy amongst fractions: he expressed the filling factor through its continued fraction representation:

$$\nu = [m, \alpha_1, p_1, \dots, \alpha_n, p_n] := \frac{1}{m + \frac{\alpha_1}{p_1 + \frac{\alpha_2}{p_2 + \frac{\dots}{p_{n-1} + \frac{\alpha_n}{p_n}}}}} \quad (3.1.1)$$

where  $m = 1, 3, 5, \dots$ ,  $\alpha_i = \pm 1$  and  $p_i = 2, 4, 6, \dots$

Then he observed the following necessary condition: for any filling fraction  $[m, \alpha_1, p_1, \dots, \alpha_n, p_n]$  to be observed it is necessary that the parent filling factor  $[m, \alpha_1, p_1, \dots, \alpha_{n-1}, p_{n-1}]$  is observed as well. A problem with this geometry is caused by the necessity to work with magnetic monopoles: in fact, since the magnetic field must be normal to the surface where the electrons are, it means that it must be oriented in the radial direction. This implies that it should somehow be generated by a magnetic monopole at the center of the sphere.

The other popular geometry is that of a flat disk. Here we cannot enjoy the comfort of an analytic ground state wavefunction or any other simplifying condition on the quantum numbers, except that given by projection on the LLL, conservation of angular momentum and the fact that it commutes with the coulombic interaction operator. Nonetheless, even in this general context, the matrix elements can be computed analytically. As we will show in the next sections, they can be used to perform numerical diagonalizations that yield exact wavefunctions for the ground and excited states of the system.

To be clear, analytical calculation of matrix elements is not something all theories for the FQHE can rely on: for example, in composite fermion theory the energy spectrum at a certain filling fraction is obtained by a process

### 3.2. ANALYTIC COULOMB INTERACTION MATRIX ELEMENTS

called CF diagonalization, which involves multi-dimensional integrals that cannot be expressed by means of any known function, even though they are mathematically well defined.

With all this in mind it is clear that the choice of a geometry must be done contextually to the goals of the analysis. We choose to work in the disk geometry in order to obtain exact wavefunctions to compare with our previous results. It is also the choice that permits us to carry out the analysis in a framework that is most similar to the experimental setup.

### 3.2 Analytic Coulomb interaction matrix elements

Our goal in this section is to find an analytic expression for the Coulomb matrix elements appearing in the many-body hamiltonian (2.3.5), namely

$$\left\langle m, n \left| \frac{1}{|z|} \right| m', n' \right\rangle \quad (3.2.1)$$

Where we employed the shorthand notation  $|m, n\rangle \equiv |0, m\rangle \otimes |0, n\rangle$ . Our result will be obtained for a system characterized by disk geometry. For our discoidal system, the single particle vectors  $|0, m\rangle$  are represented by the wavefunctions (1.2.32).

As in the three-body problem, since the eigenstates of the non-interacting system diagonalize the angular momentum, which in turn commutes with the Coulomb interaction operator, we have

$$\left\langle m, n \left| L \frac{1}{|z|} \right| m', n' \right\rangle = \hbar(m+n) \left\langle m, n \left| \frac{1}{|z|} \right| m', n' \right\rangle \quad (3.2.2)$$

$$= \hbar(m'+n') \left\langle m, n \left| \frac{1}{|z|} \right| m', n' \right\rangle \quad (3.2.3)$$

$$(3.2.4)$$

Subtracting the equalities gives

$$(m+n-m'-n') \left\langle m, n \left| \frac{1}{|z|} \right| m', n' \right\rangle = 0 \quad (3.2.5)$$

Hence if the matrix element is non-zero the first term must vanish. This condition can be parametrized by letting  $l \in \mathbb{Z}$  and fixing

$$\begin{cases} m = m' + l \\ n' = n + l \end{cases} \quad (3.2.6)$$

Hence we only need to calculate matrix elements of the form<sup>1</sup>

$$M_{mn}^l := \left\langle m+l, n \left| \frac{1}{|z|} \right| m, n+l \right\rangle \quad (3.2.7)$$

---

<sup>1</sup>We have dropped the prime from  $m'$ .

### 3. COULOMB INTERACTION IN THE DISK GEOMETRY

Using the usual coordinate representation where  $z_j = x_j - iy_j$  we have

$$M_{mn}^l = \frac{1}{\pi^2 2^{2+m+n+l} \sqrt{(m+l)!(n+l)!m!n!}} \mathcal{K}_{mn}^l \quad (3.2.8)$$

$$\mathcal{K}_{mn}^l := \int_{\mathbb{C}^2} dz_1 dz_2 z_1^{*m+l} z_2^{*n} \frac{1}{|z_1 - z_2|} z_1^m z_2^{n+l} e^{-\frac{|z_1|^2 + |z_2|^2}{2}} \quad (3.2.9)$$

Where it is intended that  $dz_j = dx_j dy_j$ . To compute  $\mathcal{K}_{mn}^l$  we start by performing the following change of variables

$$z_2 = \alpha z_1, \alpha \in \mathbb{C} \quad dz_2 = |z_1|^2 d\alpha$$

which yields:

$$\mathcal{K}_{mn}^l = \int_{\mathbb{C}^2} d\alpha dz_1 |z_1|^{2(m+n+l)+1} |\alpha|^{2n} \frac{\alpha^l}{|1-\alpha|} e^{-|z_1|^2(1+|\alpha|^2)/2} \quad (3.2.10)$$

Choosing polar coordinates for  $z_1 = \rho e^{i\phi}$  we get

$$\mathcal{K}_{mn}^l = 2\pi \int_{\mathbb{C}} d\alpha \frac{|\alpha|^{2n} \alpha^l}{|1-\alpha|} \int_0^\infty d\rho \rho^{2(1+m+n+l)} e^{-\rho^2(1+|\alpha|^2)/2}$$

Next we intend to express the second integral through a gamma function. To do this we perform the change of variable

$$u := \frac{\rho^2}{2} (1 + |\alpha|^2) \quad d\rho = \sqrt{\frac{1 + |\alpha|^2}{2u}} \frac{du}{1 + |\alpha|^2}$$

which leads us to the following:

$$\begin{aligned} \mathcal{K}_{mn}^l &= \pi \int_{\mathbb{C}} d\alpha \frac{|\alpha|^{2n} \alpha^l}{|1-\alpha|} (1 + |\alpha|^2)^{-(m+n+l+\frac{3}{2})} 2^{(m+n+l+\frac{3}{2})} \int_0^\infty du u^{m+n+l+\frac{1}{2}} e^{-u} \\ &= \pi 2^{m+n+l+\frac{3}{2}} \Gamma\left(m+n+l+\frac{3}{2}\right) \int_{\mathbb{C}} d\alpha \frac{|\alpha|^{2n} \alpha^l}{|1-\alpha|} (1 + |\alpha|^2)^{-(m+n+l+\frac{3}{2})} \end{aligned} \quad (3.2.11)$$

This takes care of the integration in  $z$ . We now focus on the integral in  $\alpha$  of Equation (3.2.11), which we call  $J_{mn}^l$ . Adopting polar coordinates  $\alpha = r e^{i\theta}$

### 3.2. ANALYTIC COULOMB INTERACTION MATRIX ELEMENTS

gives:

$$\begin{aligned}
g_{mn}^l &:= \int_{\mathbb{C}} d\alpha \frac{|\alpha|^{2n} \alpha^l}{|1-\alpha|} \left(1+|\alpha|^2\right)^{-(m+n+l+\frac{3}{2})} \\
&= \int_0^\infty dr \frac{r^{2n+l+1}}{(1+r^2)^{m+n+l+\frac{3}{2}}} \int_0^{2\pi} d\theta \frac{e^{il\theta}}{\sqrt{(1-re^{i\theta})(1-re^{-i\theta})}} \\
&= \left( \int_0^1 + \int_1^\infty \right) dr \frac{r^{2n+l+1}}{(1+r^2)^{m+n+l+\frac{3}{2}}} \int_0^{2\pi} d\theta \frac{e^{il\theta}}{\sqrt{1-2r\cos\theta+r^2}}
\end{aligned} \tag{3.2.12}$$

For the integral on  $(1, \infty)$  we change variables again choosing  $s := 1/r$ , obtaining

$$\begin{aligned}
g_{mn}^l &= \int_0^1 dr \frac{r^{2n+l+1}}{(1+r^2)^{m+n+l+\frac{3}{2}}} \int_0^{2\pi} d\theta \frac{e^{il\theta}}{\sqrt{1-2r\cos\theta+r^2}} + \\
&+ \int_0^1 ds \frac{s^{-2n-l-2}}{(1+s^{-2})^{m+n+l+\frac{3}{2}}} \int_0^{2\pi} d\theta \frac{e^{il\theta}}{\sqrt{1-2s\cos\theta+s^2}}
\end{aligned} \tag{3.2.13}$$

Since  $r$  and  $s$  are merely dummy variables and the  $\theta$  integral is the same for both addenda, the integrals in  $r$  and  $s$  can be grouped together, obtaining

$$g_{mn}^l = \int_0^1 dr \frac{r^{l+1} (r^{2m} + r^{2n})}{(1+r^2)^{m+n+l+\frac{3}{2}}} \int_0^{2\pi} d\theta \frac{e^{il\theta}}{\sqrt{1-2r\cos\theta+r^2}} \tag{3.2.14}$$

Next we observe that the angular integral is real valued, for parity reasons:

$$I_{mn}^l := \int_0^{2\pi} d\theta \frac{e^{il\theta}}{\sqrt{1-2r\cos\theta+r^2}} = \int_0^{2\pi} d\theta \frac{\cos(l\theta)}{\sqrt{1-2r\cos\theta+r^2}} \tag{3.2.15}$$

Now, this can be expressed through the use of hypergeometric functions[24]. In fact, the following relation holds (cf. Equation (9.112) from [25])

$$I_{mn}^l = \frac{2\pi}{l!} \left(\frac{1}{2}\right)_l r^l {}_2F_1\left(\frac{1}{2}, l + \frac{1}{2}, l + 1 \mid r^2\right) \tag{3.2.16}$$

where the function  ${}_2F_1$  is the Gaussian hypergeometric function and  $(x)_n$  is the Pochhammer symbol<sup>2</sup>.

<sup>2</sup>The Pochhammer symbol is defined by

$$(x)_n := \frac{\Gamma(x+n)}{\Gamma(x)}$$

### 3. COULOMB INTERACTION IN THE DISK GEOMETRY

Proceeding with the calculation, we must now deal with the radial integral

$$g_{mn}^l = \frac{2\pi}{l!} \left(\frac{1}{2}\right)_l \int_0^1 dr \frac{r^{2l+1} (r^{2m} + r^{2n})}{(1+r^2)^{m+n+l+\frac{3}{2}}} {}_2F_1\left(\frac{1}{2}, l + \frac{1}{2}, l + 1 \mid r^2\right) \quad (3.2.17)$$

Our final substitution consists in setting  $x := r^2$ , to get

$$\begin{aligned} g_{mn}^l &= \frac{2\pi}{l!} \left(\frac{1}{2}\right)_l \cdot \\ &\cdot \int_0^1 dx \left(x^{m+l} + x^{n+l}\right) (1+x)^{-(m+n+l+\frac{3}{2})} {}_2F_1\left(\frac{1}{2}, l + \frac{1}{2}, l + 1 \mid x\right) \end{aligned} \quad (3.2.18)$$

Thanks to linearity, this can be split into two addenda that are completely symmetric under the exchange of  $m$  and  $n$ . Hence we can focus on either one of them, indifferently. For reasons that will be clear in a while we employ the following trick:

$$\begin{aligned} x^{m+l}(1+x)^{-(m+n+l+\frac{3}{2})} &= x^l(1+x-1)^m(1+x)^{-(m+n+l+\frac{3}{2})} \\ &= x^l \sum_{k=0}^m \binom{m}{k} (-1)^k (1+x)^{m-k-m-n-l-\frac{3}{2}} \end{aligned}$$

Applying this to our integral we obtain

$$\begin{aligned} &\int_0^1 dx x^{m+l}(1+x)^{-(m+n+l+\frac{3}{2})} {}_2F_1\left(\frac{1}{2}, l + \frac{1}{2}, l + 1 \mid x\right) \\ &= \sum_{k=0}^m (-1)^k \binom{m}{k} \int_0^1 dx x^l (1+x)^{-(k+n+l+\frac{3}{2})} {}_2F_1\left(\frac{1}{2}, l + \frac{1}{2}, l + 1 \mid x\right) \end{aligned} \quad (3.2.19)$$

Now, this last integral inside the sum (let's call it  $\mathcal{G}_{kn}^l$ ) can be solved exactly by employing generalized hypergeometric functions, in particular  ${}_3F_2$ . Setting

$$\gamma := l + 1, \quad \rho := 1, \quad z := -1, \quad \sigma := k + n + l + \frac{3}{2}, \quad \alpha := \frac{1}{2}, \quad \beta := l + \frac{1}{2}$$

and applying result (7.512.9) of [25] yields:

$$\mathcal{G}_{kn}^l = \frac{\Gamma(l+1)}{\Gamma\left(l + \frac{3}{2}\right) \Gamma\left(\frac{3}{2}\right) 2^{k+n+l+\frac{3}{2}}} {}_3F_2\left(\begin{matrix} 1 & k+n+l+\frac{3}{2} & 1 \\ l+\frac{3}{2} & \frac{3}{2} \end{matrix} \mid \frac{1}{2}\right) \quad (3.2.20)$$

### 3.3. EXACT DIAGONALIZATION FOR FINITE CLUSTER

Substituting these results in (3.2.18) we find

$$g_{mn}^l = \frac{\pi}{l!} \left(\frac{1}{2}\right)_l \left[ \sum_{k=0}^m (-1)^k \binom{m}{k} \mathcal{G}_{kn}^l + \sum_{j=0}^n (-1)^j \binom{n}{j} \mathcal{G}_{jm}^l \right] \quad (3.2.21)$$

Rearranging and inserting contributions from all constants and integrals we find our final result:

$$M_{mn}^l = \left(\frac{1}{2}\right)_l \left(\frac{3}{2}\right)_{m+n+l} \frac{C_{mn}^l + C_{nm}^l}{2^{l+2} \Gamma\left(l + \frac{3}{2}\right) \sqrt{(m+l)!(n+l)!m!n!}} \quad (3.2.22)$$

$$C_{mn}^l := \sum_{k=0}^m (-1)^k \binom{m}{k} 2^{-k-n} {}_3F_2\left( \begin{matrix} 1 & k+n+l+\frac{3}{2} & 1 \\ l+\frac{3}{2} & \frac{3}{2} \end{matrix} \middle| \frac{1}{2} \right) \quad (3.2.23)$$

A few observations about this result are due. First of all, the symmetry under exchange of  $m$  and  $n$  that appears in (3.2.7) is explicitly preserved in the final expression. Moreover, for cases in which  $l < 0$ , the following identity holds

$$M_{mn}^{-l} = M_{m-l, n-l}^l \quad (3.2.24)$$

A feature of result (3.2.22) is that it only involves finite sums. This makes it particularly suited to be employed in numerical calculations, as it is easily computable. Tsiper has found an equivalent result [26] only containing  $\Gamma$  functions which makes it even better for efficient numerical experiments. We give it here for future reference, because our exact diagonalization analysis employs it.

$$M_{mn}^l = \sqrt{\frac{(m+l)!(n+l)!}{m!n!}} \frac{\Gamma\left(m+n+l+\frac{3}{2}\right)}{\pi 2^{m+n+l+2}} \left( A_{mn}^l B_{nm}^l + B_{mn}^l A_{nm}^l \right) \quad (3.2.25)$$

where the coefficients  $A_{mn}^l$  and  $B_{mn}^l$  are defined by the following finite sums

$$A_{mn}^l := \sum_{i=0}^m \binom{m}{i} \frac{\Gamma\left(\frac{1}{2}+i\right) \Gamma\left(\frac{1}{2}+l+i\right)}{(l+i)! \Gamma\left(\frac{3}{2}+n+l+i\right)} \quad (3.2.26)$$

$$B_{mn}^l := \sum_{i=0}^m \binom{m}{i} \left(\frac{1}{2}+l+2i\right) \frac{\Gamma\left(\frac{1}{2}+i\right) \Gamma\left(\frac{1}{2}+l+i\right)}{(l+i)! \Gamma\left(\frac{3}{2}+n+l+i\right)} \quad (3.2.27)$$

### 3.3 Exact diagonalization for finite cluster

Having an analytical expression for the Coulomb operator matrix elements permits us to carry out the exact diagonalization of the hamiltonian (2.3.5). This analysis aims at obtaining the excitation spectrum of the FQHE system in the disk geometry for a small cluster of electrons.

### 3. COULOMB INTERACTION IN THE DISK GEOMETRY

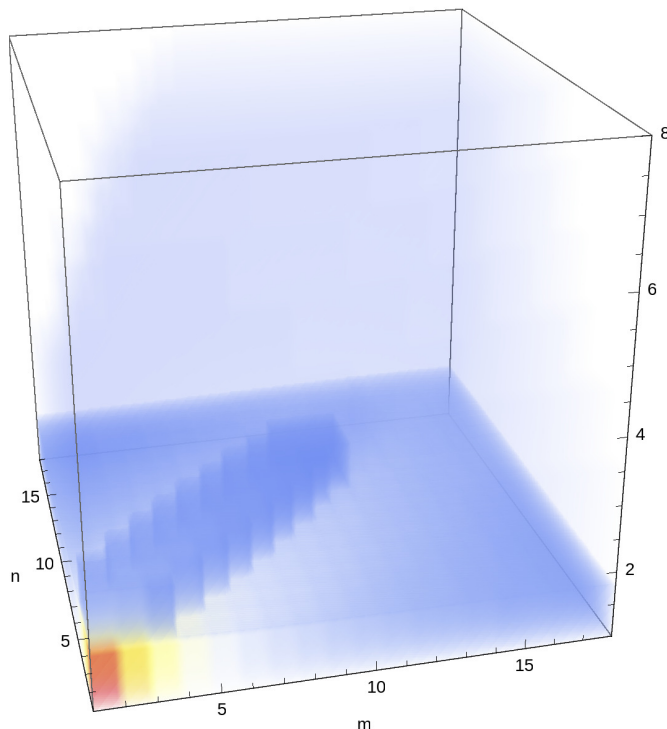


**Figure 3.1:** Representation of the matrix elements (3.2.22). Red and yellow colors represent regions of the  $m, n, l$  space where the matrix elements are large. As their values decrease the colors are shifted towards blue and finally fade out into white. The symmetry under exchange of  $m$  and  $n$  is evident from the plot. Also we observe that an increase in  $l$  causes a more considerable decrease than that caused by an increase in  $m$  or  $n$  of the same amount.

#### 3.3.1 Framework

The first step in conducting a numerical analysis rests in setting the problem in a framework in which it is solvable and organizing it to make the computation efficient. With this in mind, we rewrite the hamiltonian (2.3.5) using the parametrization (3.2.6) for the single particle angular momentum quantum numbers:

$$\hat{\mathcal{H}} = \frac{1}{2} \sum_{m=0}^{\infty} \sum_{n=0}^{\infty} \sum_{l=\lambda_{mn}}^{\infty} \left\langle m+l, n \left| \frac{1}{|z|} \right| m, n+l \right\rangle \hat{a}_{m+l}^{\dagger} \hat{a}_n^{\dagger} \hat{a}_{n+l} \hat{a}_m \quad (3.3.1)$$

$$= \frac{1}{2} \sum_{m=0}^{\infty} \sum_{n=0}^{\infty} \sum_{l=\lambda_{mn}}^{\infty} M_{mn}^l \hat{a}_{m+l}^{\dagger} \hat{a}_n^{\dagger} \hat{a}_{n+l} \hat{a}_m \quad (3.3.2)$$

where  $\lambda_{mn} := \max(-m, -n)$ . Now, one obvious obstacle in diagonalizing this operator is that it involves infinite sums. In particular the sum indices going to infinity are single particle angular momentum quantum numbers.

### 3.3. EXACT DIAGONALIZATION FOR FINITE CLUSTER

But from our study of uncorrelated electrons in magnetic field of Section 1.2 we know that angular momentum in this context quantifies the spacial extension of the electronic states on the surface. So, working with angular momentum going to infinity is equivalent to working on an infinite plane.

To overcome this practical obstacle we fix a maximum value  $L$  for single particle angular momentum quantum numbers. By doing this we also realize a much more realistic scenario from the experimental point of view. In fact a typical setup to study the FQHE is a flat surface with linear dimensions of a fraction of a millimeter. Applying this condition, the resulting hamiltonian is:

$$\hat{\mathcal{H}} = \frac{1}{2} \sum_{m=0}^L \sum_{n=0}^L \sum_{l=\lambda_{mn}}^{\kappa_{mn}} M_{mn}^l \hat{a}_{m+l}^\dagger \hat{a}_n^\dagger \hat{a}_{n+l} \hat{a}_m \quad (3.3.3)$$

where  $\kappa_{mn} := L - \max(m, n)$ .

A convenient choice of basis for the state space is that of occupation numbers. If we fix the number of particles to  $N$  this is composed by the state vectors:

$$\mathcal{B} := \left\{ |n_0 \cdots n_L\rangle : n_j \in \{0, 1\} \forall j = 0, \dots, L; \sum_{j=0}^L n_j = N \right\} \quad (3.3.4)$$

where  $n_j$  can only be zero or one because the involved particles are fermions. Note that we must fix a finite number of electrons. This is a result of choosing a cutoff value  $L$  for single particle angular momentum quantum numbers: in fact because of Pauli's principle there can be at most one particle having a certain angular momentum  $m_j$ . Since the possible values for  $m_j$  range from 0 to  $L$ , the maximum possible number of electrons is  $N_{\max} = L + 1$ .

Now, in this basis, the hamiltonian (3.3.3) is represented by a matrix whose entries are given by

$$\langle n'_0 \cdots n'_L | \hat{\mathcal{H}} | n_0 \cdots n_L \rangle \quad (3.3.5)$$

The fact that the system has a finite size, because it implies that the number of electrons must be finite, causes the total angular momentum

$$\hat{M} = \sum_{m=0}^L m \hat{a}_m^\dagger \hat{a}_m \quad (3.3.6)$$

to be conserved. This simplifies the problem significantly: in fact it implies that the hamiltonian (3.3.3) in its matrix representation and with our choice of basis is block diagonal. This is because all matrix elements (3.3.5) with

$$\hat{M} |n'_0 \cdots n'_L\rangle = M' |n'_0 \cdots n'_L\rangle, \quad \hat{M} |n_0 \cdots n_L\rangle = M |n_0 \cdots n_L\rangle \quad (3.3.7)$$

vanish identically every time  $M \neq M'$ . Hence, we can diagonalize separately all the blocks characterized by different values of total angular momentum.

### 3. COULOMB INTERACTION IN THE DISK GEOMETRY

Each block has a fixed  $M$  and the corresponding Hilbert space is a subspace of the one spanned by  $\mathcal{B}$  in which all the state vectors have  $M$  total angular momentum. A basis for this subspace is given by:

$$\mathcal{B}_M := \left\{ |n_0 \cdots n_L\rangle \in \mathcal{B} : \sum_{j=0}^L j n_j \equiv M \right\} \quad (3.3.8)$$

A simple example is helpful: in the case of  $N = 3$  electrons, with a maximum single particle angular momentum of  $L = 8$  and with the total angular momentum of the many-body states fixed to  $M = 9$ , our choice of basis for the state space amounts to:

$$\mathcal{B}_9 = \{ |110000001\rangle, |101000010\rangle, |100100100\rangle, |100011000\rangle, \\ |011000100\rangle, |010101000\rangle, |001110000\rangle \} \quad (3.3.9)$$

In this case the Hilbert subspace dimension is 7. Consider the difference in dimension of state space with and without the restriction on  $M$ . With the same parameters, the unrestricted basis  $\mathcal{B}$  would count a number of vectors given by  $\binom{L+1}{N} = 84$ , i.e. the number of different ways we can switch  $N$  zeros to ones in a string made by  $L + 1$  zeros.

Since diagonalizing a few small matrices is computationally less intensive than diagonalizing a single huge matrix, the problem is reduced to a more practical form. Moreover, if we are able to know in advance the value of  $M$  that identifies the block with the smallest eigenvalue we only need to diagonalize that one to get the ground state. However, if one wants to compute the entire excitation spectrum of the system he has to diagonalize all of the blocks.

There is no known closed form to express the dimension of the Hilbert space with fixed  $M$ . However it can be obtained computationally with ease. Kasner and Apel have also reported that it can be obtained from the coefficients of the power series representation of a generating function[27].

To build the hamiltonian we must compute the matrix elements (3.3.5). We already know the coefficients  $M_{mn}^l$ , so the only remaining part is the quantity

$$K_{mn}^l(\{n'\}, \{n\}) := \langle n'_0 \cdots n'_L | \hat{a}_{m+l}^\dagger \hat{a}_n^\dagger \hat{a}_{n+l} \hat{a}_m | n_0 \cdots n_L \rangle \quad (3.3.10)$$

We calculate this making use of the following relation, which expresses the action of a fermionic annihilation operator on occupation number state vectors:

$$\hat{a}_\lambda |n_0 \cdots n_L\rangle = \delta_1^{n_\lambda} (-1)^{\sigma_\lambda} |n_0 \cdots (n_\lambda - 1) \cdots n_L\rangle, \quad \sigma_\lambda := \sum_{j=0}^{\lambda-1} n_j \quad (3.3.11)$$

### 3.3. EXACT DIAGONALIZATION FOR FINITE CLUSTER

Applying this to (3.3.10), if the  $\hat{a}$  operators act on the right and the  $\hat{a}^\dagger$  operators act on their left we get<sup>3</sup>

$$K_{mn}^l (\{n'\}, \{n\}) = \quad (3.3.12)$$

$$= \delta_1^{n_m} (-1)^{\sigma_m} \langle n'_0 \cdots n'_L \mid \hat{a}_{m+l}^\dagger \hat{a}_n^\dagger \hat{a}_{n+l} \mid n_0 \cdots (n_m - 1) \cdots n_L \rangle \quad (3.3.13)$$

$$= \delta_1^{n_m} \delta_1^{n_{n+l}} (-1)^{\sigma_m + \tilde{\sigma}_{n+l}} \cdot \langle n'_0 \cdots n'_L \mid \hat{a}_{m+l}^\dagger \hat{a}_n^\dagger \mid n_0 \cdots (n_m - 1) \cdots (n_{n+l} - 1) \cdots n_L \rangle \quad (3.3.14)$$

$$= \delta_1^{n_m} \delta_1^{n_{n+l}} \delta_1^{n'_{m+l}} \delta_1^{n'_n} (-1)^{\sigma_m + \tilde{\sigma}_{n+l} + \sigma'_{m+l} + \tilde{\sigma}'_n} \cdot \langle n'_0 \cdots (n'_n - 1) \cdots (n'_{m+l} - 1) \cdots n'_L \mid n_0 \cdots (n_m - 1) \cdots (n_{n+l} - 1) \cdots n_L \rangle \quad (3.3.15)$$

We have used the prime over  $\sigma_\lambda$  to indicate that it must be computed using the  $\{n'\}$  occupation numbers. Also, a tilde appears in  $\tilde{\sigma}_\lambda$  or  $\tilde{\sigma}'_\lambda$  whenever the quantity must be calculated on those vectors on which an annihilation operator has already acted. The last bracket product is left indicated, as it is promptly computed case by case by the diagonalization program: in any case it evaluates to another product of Kronecker deltas.

Using this result, the hamiltonian matrix element (3.3.5) evaluates to

$$\langle n'_0 \cdots n'_L \mid \hat{\mathcal{H}} \mid n_0 \cdots n_L \rangle = \frac{1}{2} \sum_{m=0}^L \sum_{n=0}^L \sum_{l=\lambda_{mn}}^{\kappa_{mn}} M_{mn}^l K_{mn}^l (\{n'\}, \{n\}) \quad (3.3.16)$$

Now, the core of the exact diagonalization problem is in how we choose the values of  $L$  and  $M$  to analyze. Ideally, since the hamiltonian is block diagonal, if we knew where to look it would be very easy to find the ground state.

The value of  $L$  is fixed by the cluster size  $N$  and the filling fraction  $\nu$ . In particular its value can be specified by considering the following expression for the filling fraction:

$$\nu = 2\pi \frac{N}{S} = \frac{2N}{R_0^2} = \frac{N}{L + \frac{1}{2}} \quad (3.3.17)$$

If we restrict our analysis to the case of Laughlin type filling fractions  $\nu = 1/2k + 1$ , with  $k = 0, 1, 2, \dots$  we get

$$L = \left\lfloor (2k + 1)N - \frac{1}{2} \right\rfloor = (2k + 1)N - 1 \quad (3.3.18)$$

Sometimes it is more fruitful to use another expression for the filling fraction:

$$\nu' = \frac{N - 1}{L} \quad (3.3.19)$$

---

<sup>3</sup>We use the letter  $n$  as an index as well as the symbol for occupation numbers in general. This will not cause any confusion.

### 3. COULOMB INTERACTION IN THE DISK GEOMETRY

This definition is completely equivalent to (3.3.17) in the thermodynamic limit and it leads to the alternative value of

$$L = (2k + 1)(N - 1) \tag{3.3.20}$$

A hint for the value of  $M$  comes from Laughlin's wavefunction, which is an eigenfunction of total angular momentum with eigenvalue

$$M = (2k + 1)\frac{N(N - 1)}{2}$$

as is clear by considering that each distinct couple of electrons carries an angular momentum  $2k + 1$ . This tells us that choosing  $M$  as above in the thermodynamic limit of  $N \rightarrow \infty$  gives the inverse filling fraction  $2k + 1$ . Still, we are working with small clusters of electrons and we are nowhere near the thermodynamic limit. So this value of  $M$  as a finite  $N$  approximation must be checked by our analysis.

#### 3.3.2 Numerical study

Amongst our goals is that of comparing the exact ground states that we find with Laughlin's wavefunction. Now, usually when an exact diagonalization result is compared with Laughlin's state, the wavefunction of the latter is constructed as the ground state of the first Haldane pseudopotential [23] in the same restricted space as the exact ground state. In our case, we have constructed it decomposing Laughlin's ansatz in Slater determinants following Dunne [4]. For the  $N = 3$  problem the decomposition is easy to obtain, but as the number of involved particles increases, calculating the coefficient corresponding to any particular term becomes extremely challenging. An algorithm that delivers this result was perfected by Haldane and Bernevig [5] but is quite convoluted and computationally intensive, especially starting from 5 particles onwards. From the decomposition in Slater determinants it is trivial to obtain the expression of Laughlin's state in the basis of occupation numbers.

To search for the ground state we diagonalize the blocks with total angular momentum ranging from  $M = L + 1$  to  $M = N(2L - N + 1)/2$  and look for the minimum energy eigenvalue. We also study how the results change by varying  $L$  (which amounts to tweaking the filling factor). We find that by increasing  $L$  the exact ground state angular momentum grows as well.

Our analysis was carried out making use of a computer program we wrote in C++, which makes use of the Eigen library<sup>4</sup>, vastly popular for scientific purposes.

We start by studying the case of  $N = 3$ . Using (3.3.17) with  $\nu = 1/3$ , the value of maximum single particle angular momentum is  $L = 8$ . In Figure 3.2

---

<sup>4</sup>Eigen is Free Software. Think of it as "free as in free speech not as in free beer". To learn more visit The Free Software Foundation or The GNU Project.

### 3.3. EXACT DIAGONALIZATION FOR FINITE CLUSTER

we plot the ground state energy as a function of total angular momentum. The lowest energy is found at  $M = 18$ , while Laughlin's state has  $M = 9$ . As we wish to compare the exact ground state with Laughlin's wavefunction, this is unsettling because states with different total angular momenta and same number of particles are necessarily orthogonal.

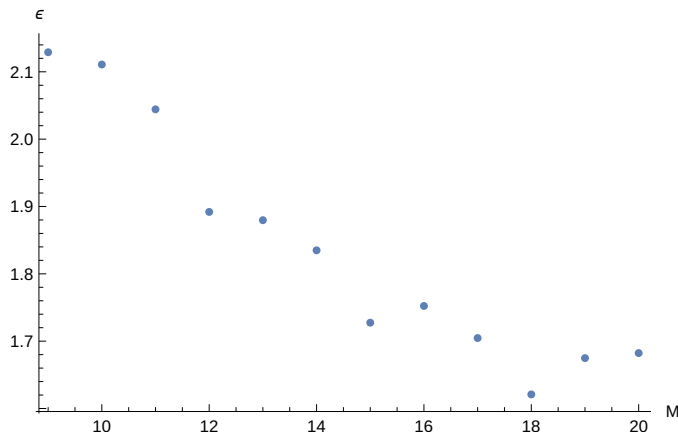


**Figure 3.2:** Ground state energy  $\epsilon$  as a function of total angular  $M$  for the case of  $N = 3$  particles with maximum single particle angular momentum  $L = 8$ . The true ground state is found to be at  $M = 18$ .

To try and find a solution to this problem we insert in the hamiltonian (3.3.3) an additional neutralizing background term. This is different from what we did in the case of three particles: in fact, there we put the electrons in a potential well to mimic the band energy. Here we are realizing a form of homogeneous electron gas (HEG), which is a popular model for interacting electrons in many-body theory. It consists in setting the electrons on a positively charged layer, which neutralizes the negative charge. This layer is usually taken to be uniformly charged, hence the name HEG.

We realize this model by inserting on our disk  $N$  additional single particle wavefunctions (1.2.32) relative to fermions of charge  $+e$ . Note that by doing so we are not precisely introducing a uniform background. However the background becomes uniform in the thermodynamic limit. The total hamiltonian must also account for the interaction energies of the background with itself and with the electrons. If we take complex numbers  $\{w_j\}$  to represent the positions of the positive charges, the two additional terms are

$$V_{+/+} = e^2 \sum_{i < j} \frac{1}{|w_i - w_j|} \quad (3.3.21)$$

$$V_{+/-} = -e^2 \sum_{i=1}^N \sum_{j=1}^N \frac{1}{|z_i - w_j|} \quad (3.3.22)$$

### 3. COULOMB INTERACTION IN THE DISK GEOMETRY

The first one is the self interaction of the background. As such, it does not involve any electronic wavefunction, so from the point of view of the electrons is a zero-particle interaction, which amounts to a constant. The second term represents the electron-background binding term which decreases the total energy. Because the positive and negative fermions can be distinguished from one another, the sums here are independent. From the point of view of the electrons, this is a sum of one-particle interactions.

The resulting interaction to be added to the hamiltonian (3.3.3) is obtained by taking the sum of the second quantized form of the operators (3.3.22):

$$\hat{\mathcal{H}}_{\text{HEG}} := -\nu \sum_{m=0}^L \sum_{l=-m}^{L-m} M_{mm}^l \hat{a}_m^\dagger \hat{a}_m + \frac{\nu^2}{2} \sum_{m=0}^L \sum_{l=-m}^{L-m} M_{mm}^l \quad (3.3.23)$$

$$= \frac{\nu}{2} \sum_{m=0}^L \sum_{l=-m}^{L-m} M_{mm}^l (\nu - 2m) \quad (3.3.24)$$

This background term has the effect to promote states with lower total angular momenta. If we repeat the analysis with this additional potential we find the results of Figure 3.3: this time the exact ground state is found

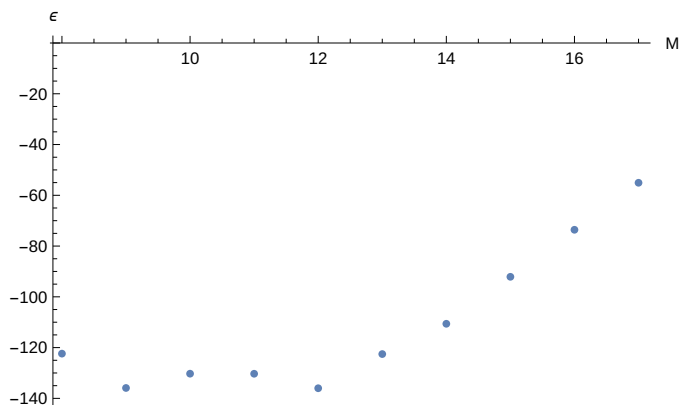


**Figure 3.3:** Ground state energy  $\epsilon$  as a function of total angular  $M$  for the case with background potential switched on,  $N = 3$  particles with maximum single particle angular momentum  $L = 8$ . This time the true ground state is found to be at  $M = 9$ .

to have the same total angular momentum as Laughlin's state.

We outline the relationship between the ground states of the hamiltonian with and without background potential as follows. Laughlin's wavefunction is the exact ground state of the short range interaction expressed by Haldane's first pseudopotential. It resembles the true ground state of the FQHE system more and more as the thermodynamic limit is approached. Moreover, because the Coulomb interaction is long range, if Laughlin's wavefunction approximates well the exact ground state, it must be that in the presence of

### 3.3. EXACT DIAGONALIZATION FOR FINITE CLUSTER

a large number of particles the effective interaction has a short range. We take the ground state of the hamiltonian with background potential merely as an indicator of which state (identified by values of  $L$  and  $M$ ) will be preferred as a ground state as the number of electrons is increased. We will then use the ground states identified by  $L$  and  $M$  of the hamiltonian with the background potential switched off to compare them with Laughlin's wavefunction.

Operating in this way for the case  $N = 3$ ,  $L = 8$  and  $M = 9$  we find a normalized overlap between the exact FQHE ground state of

$$\left| \langle \Psi^{(L)} | \Psi^{(E)} \rangle \right| = 0.997438 \quad (3.3.25)$$

where L stands for Laughlin and E for Exact. The overlap is particularly good as we can also see from Figure 3.4 in which we plot the radial charge densities associated with Laughlin's wavefunction and with our exact ground state.

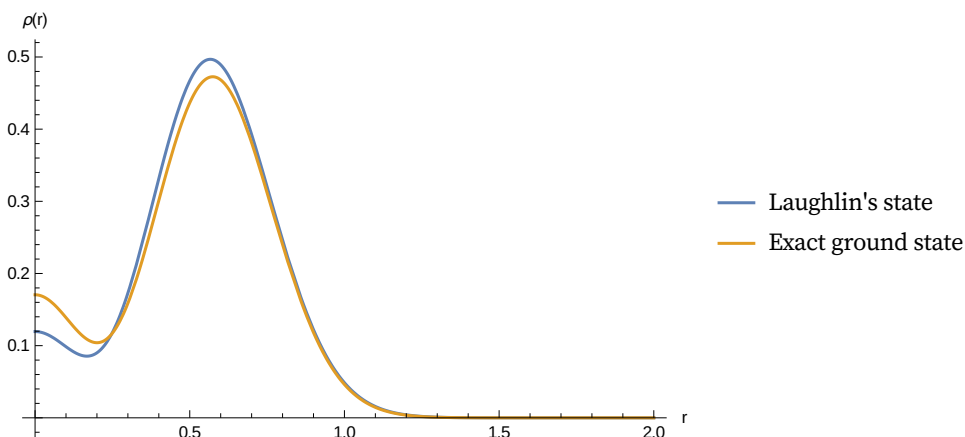


**Figure 3.4:** Comparison for  $\nu = 1/3$  and  $N = 3$  of charge densities obtained from Laughlin's wavefunction and the exact ground state wavefunction. The radial coordinate  $r$  is measured in units of magnetic length  $\ell$ .

We ran the same analysis for the case of  $N = 4$  particles. This time we used the relation involving  $\nu'$  to fix the  $L$  quantum number. With 4 electrons and at filling factor  $1/3$  Laughlin's wavefunction has total angular momentum quantum number 18. The exact ground state for the interaction without background potential has  $M = 21$ , as shown in Figure 3.5. Hence it is incompatible with Laughlin's theory. Similarly to the case with 3 particles, however, switching on the background potential promotes ground states with lower total angular momentum: in particular the exact ground state for the case with background potential switched on is characterized by  $M = 18$ , compatible with Laughlin's state.

However in this case the normalized overlap between the two wavefunc-

### 3. COULOMB INTERACTION IN THE DISK GEOMETRY

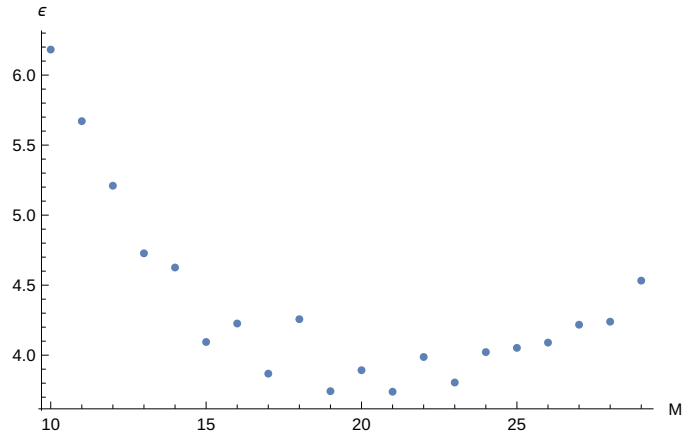


**Figure 3.5:** The ground state energies for the case of  $N = 4, L = 9$  with background interaction switched off. The minimum is found at  $M = 21$ .

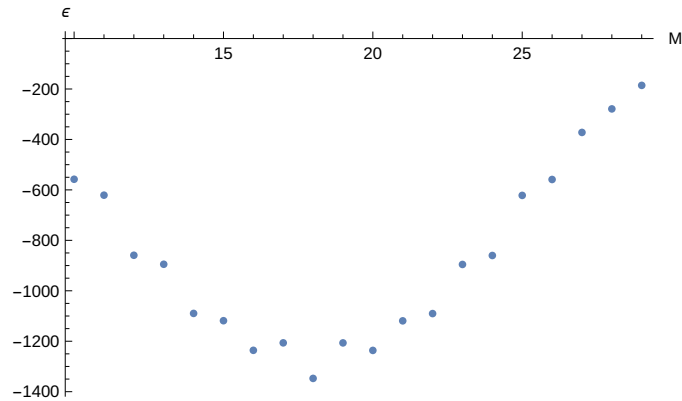


**Figure 3.6:** The ground state energies for the case of  $N = 4, L = 9$  with background interaction. The total angular momenta are shifted downwards and now the minimum at  $M = 18$  agrees with that of Laughlin's wavefunction.

tion is not as good as in the previous case (3.3.25):

$$\left| \langle \Psi^{(L)} | \Psi^{(E)} \rangle \right| = 0.627147 \quad (3.3.26)$$

#### 3.3.3 Remarks

The result for four electrons is clearly worse than that of three: this actually anticipates a problem that is found in a more fundamental way for the cases of 5, 6, 7 and 8 electrons. In those cases there appears to be no exact ground state with angular momenta compatible with Laughlin's state. To clarify, in both the cases we studied we observed that there is a unique value of  $L$  that yields a ground state with a value of  $M$  compatible with Laughlin's wavefunction. Also, that value of  $L$  agrees with either one of the filling

### 3.3. EXACT DIAGONALIZATION FOR FINITE CLUSTER

factor definitions (3.3.17) or (3.3.19). Moreover, the ground states have always resulted to be nondegenerate.

This nondegeneracy is important for a number of reasons: first of all, because (in the thermodynamic limit) Laughlin's wavefunction is the nondegenerate ground state for the FQHE condensate. Hence our exact result agrees on this level with Laughlin's ansatz. Moreover, a crucial information we can extract from the excitation spectra shown before is the size of the energy gaps. In particular we are interested in the energy gap between the ground state and the first excited state. We observe that it is fairly small for the three particles, but starts to get large when  $N = 4$ . The presence of a large energy gap is central to the phenomenology of the FQHE, as it causes the system to not be easily prone to excitations, which would otherwise modify the resistance.

Because of the way we obtain it, the Laughlin state we work with is defined on the whole plane, even though the system we are studying is finite. Maybe by applying some finite size corrections to Laughlin's wavefunction the compatibility with the exact ground state might improve. Still it must be kept in mind that Laughlin's ansatz validity holds best in the thermodynamic limit, which our system certainly does not approximate well.

Still, the question remains as why the compatibility is particularly good for the case of three particles but so bad for the next values of  $N$ . Anyhow, it has been shown that, in the disk geometry, a more appropriate interaction to model the FQHE for finite clusters of electrons is the short range interaction without any background potential, instead of the Coulomb interaction [27]. In that case, in fact, the compatibility with Laughlin's state has been shown to be preserved independently of the number of particles for up to 9 electrons.

This substantial difference between Coulomb and short range interaction disappears, at least qualitatively, in the spherical geometry. This probably indicates that the cause of this discrepancy between the two models is to be accounted to edge effects, which do not present themselves in the case of spherical geometry.

This page intentionally left blank.

# Conclusions

In this work we analyze the FQHE from two different perspectives: we start by inspecting the problem of three electrons with first-quantized formalism as a source of insight for the real many-body system, on which we focus next.

We solve the three-body problem exactly. This is made possible by restricting the analysis to the lowest Landau level. In this context we find the full excitation spectrum and illustrate how the ground state of the cluster is incompressible.

This result is indeed interesting, because in the many-body framework the ground state of the system is approximated extremely well by Laughlin's wavefunction, which at filling factors  $1/q$  (with  $q \leq 70$ ) describes an incompressible homogeneous fluid. This qualitative feature of incompressibility thus represents an important connection between the FQHE ground states in the two different frameworks.

Next we consider a FQH system with disk geometry and for it we derive an analytical expression for the Coulomb interaction matrix elements in terms of finite sums. An equivalent expression of these quantities is then employed to conduct an exact diagonalization of the hamiltonian for a small cluster of electrons. We found non-degenerate ground states presenting appreciable energy gaps, central to the FQHE phenomenology. The comparison of the exact ground states with Laughlin's wavefunction unveiled the importance of edge effects for finite systems in the disk geometry. These constitute an issue that does not present itself in geometries with periodic properties.

This last part of the study leaves some open questions, concerning the compatibility of Laughlin's wavefunction with exact ground states in the finite disk geometry for clusters of 5-8 electrons and the relationship between Haldane's short range interaction and Coulomb's interaction.

This page intentionally left blank.

## Appendix A

# Three particles matrix elements

Below are reported the first 19 matrices of the coulomb operator, in units of  $3e^2/\ell\sqrt{2}$ .

$$\begin{aligned} & \left( \frac{29\sqrt{\frac{\pi}{2}}}{64} \right) & (M = 3) \\ & \left( \frac{1627\sqrt{\frac{\pi}{2}}}{4096} \right) & (M = 5) \\ & \left( \frac{1373\sqrt{\frac{\pi}{2}}}{4096} \right) & (M = 6) \\ & \left( \frac{46761\sqrt{\frac{\pi}{2}}}{131072} \right) & (M = 7) \\ & \left( \frac{21085\sqrt{\frac{\pi}{2}}}{65536} \right) & (M = 8) \\ & \left( \begin{array}{cc} \frac{4553723\sqrt{\frac{\pi}{2}}}{16777216} & \frac{19077\sqrt{\frac{21\pi}{2}}}{8388608} \\ \frac{19077\sqrt{\frac{21\pi}{2}}}{8388608} & \frac{1367831\sqrt{\frac{\pi}{2}}}{4194304} \end{array} \right) & (M = 9) \\ & \left( \frac{5178219\sqrt{\frac{\pi}{2}}}{16777216} \right) & (M = 10) \\ & \left( \begin{array}{cc} \frac{142538921\sqrt{\frac{\pi}{2}}}{536870912} & \frac{1560567\sqrt{15\pi}}{536870912} \\ \frac{1560567\sqrt{15\pi}}{536870912} & \frac{81063847\sqrt{\frac{\pi}{2}}}{268435456} \end{array} \right) & (M = 11) \\ & \left( \begin{array}{cc} \frac{62702273\sqrt{\frac{\pi}{2}}}{268435456} & \frac{242895\sqrt{\frac{55\pi}{2}}}{268435456} \\ \frac{242895\sqrt{\frac{55\pi}{2}}}{268435456} & \frac{79560695\sqrt{\frac{\pi}{2}}}{268435456} \end{array} \right) & (M = 12) \\ & \left( \begin{array}{cc} \frac{4463216685\sqrt{\frac{\pi}{2}}}{17179869184} & \frac{83862675\sqrt{33\pi}}{34359738368} \\ \frac{83862675\sqrt{33\pi}}{34359738368} & \frac{9702956493\sqrt{\frac{\pi}{2}}}{34359738368} \end{array} \right) & (M = 13) \end{aligned}$$

A. THREE PARTICLES MATRIX ELEMENTS

$$\left( \begin{array}{cc} \frac{986501059\sqrt{\frac{\pi}{2}}}{4294967296} & \frac{11543421\sqrt{143\pi}}{17179869184} \\ \frac{11543421\sqrt{143\pi}}{17179869184} & \frac{9795308429\sqrt{\frac{\pi}{2}}}{34359738368} \end{array} \right) \quad (M = 14)$$

$$\left( \begin{array}{ccc} \frac{228904177941\sqrt{\frac{\pi}{2}}}{1099511627776} & \frac{208281515\sqrt{\frac{455\pi}{2}}}{1099511627776} & \frac{11449333\sqrt{\frac{5005\pi}{2}}}{1099511627776} \\ \frac{208281515\sqrt{\frac{455\pi}{2}}}{1099511627776} & \frac{279565302739\sqrt{\frac{\pi}{2}}}{1099511627776} & \frac{7504047565\sqrt{\frac{11\pi}{2}}}{1099511627776} \\ \frac{11449333\sqrt{\frac{5005\pi}{2}}}{1099511627776} & \frac{7504047565\sqrt{\frac{11\pi}{2}}}{1099511627776} & \frac{292574872017\sqrt{\frac{\pi}{2}}}{1099511627776} \end{array} \right) \quad (M = 15)$$

$$\left( \begin{array}{cc} \frac{62140764963\sqrt{\frac{\pi}{2}}}{274877906944} & \frac{280185993\sqrt{\frac{455\pi}{2}}}{549755813888} \\ \frac{280185993\sqrt{\frac{455\pi}{2}}}{549755813888} & \frac{151028152125\sqrt{\frac{\pi}{2}}}{549755813888} \end{array} \right) \quad (M = 16)$$

$$\left( \begin{array}{ccc} \frac{57777681176451\sqrt{\frac{\pi}{2}}}{281474976710656} & \frac{171662211709\sqrt{\frac{35\pi}{2}}}{140737488355328} & \frac{11991788675\sqrt{143\pi}}{140737488355328} \\ \frac{171662211709\sqrt{\frac{35\pi}{2}}}{140737488355328} & \frac{17515322652905\sqrt{\frac{\pi}{2}}}{70368744177664} & \frac{17343508093\sqrt{5005\pi}}{70368744177664} \\ \frac{11991788675\sqrt{143\pi}}{140737488355328} & \frac{17343508093\sqrt{5005\pi}}{70368744177664} & \frac{8876098108845\sqrt{\frac{\pi}{2}}}{35184372088832} \end{array} \right) \quad (M = 17)$$

$$\left( \begin{array}{ccc} \frac{53379983866091\sqrt{\frac{\pi}{2}}}{281474976710656} & \frac{12834571655\sqrt{\frac{51\pi}{2}}}{35184372088832} & \frac{982253305\sqrt{\frac{4641\pi}{2}}}{140737488355328} \\ \frac{12834571655\sqrt{\frac{51\pi}{2}}}{35184372088832} & \frac{979238156329\sqrt{\frac{\pi}{2}}}{4398046511104} & \frac{34646642935\sqrt{\frac{91\pi}{2}}}{17592186044416} \\ \frac{982253305\sqrt{\frac{4641\pi}{2}}}{140737488355328} & \frac{34646642935\sqrt{\frac{91\pi}{2}}}{17592186044416} & \frac{18664220010163\sqrt{\frac{\pi}{2}}}{70368744177664} \end{array} \right) \quad (M = 18)$$

$$\left( \begin{array}{ccc} \frac{1824430304205045\sqrt{\frac{\pi}{2}}}{9007199254740992} & \frac{11182008347211\sqrt{\frac{17\pi}{2}}}{4503599627370496} & \frac{934663185429\sqrt{221\pi}}{9007199254740992} \\ \frac{11182008347211\sqrt{\frac{17\pi}{2}}}{4503599627370496} & \frac{548844907077573\sqrt{\frac{\pi}{2}}}{2251799813685248} & \frac{23066331838683\sqrt{13\pi}}{4503599627370496} \\ \frac{934663185429\sqrt{221\pi}}{9007199254740992} & \frac{23066331838683\sqrt{13\pi}}{4503599627370496} & \frac{1082514117068865\sqrt{\frac{\pi}{2}}}{4503599627370496} \end{array} \right) \quad (M = 19)$$

The coulomb matrix eigenvalues have been computed numerically and are presented in the following table:

$M$	Eigenvalues ( $10^{-1} \cdot 3e^2/\ell\sqrt{2}$ )		
3	5.67908		
5	4.97837		
6	4.20117		
7	4.4713		
8	4.03231		
9	4.11131	3.37774	
10	3.8683		
11	3.85966	3.25272	
12	3.72354	2.91866	
13	3.68369	3.11162	
14	3.60104	2.85063	
15	3.55564	2.9709	2.60443
16	3.49887	2.77754	
17	3.45685	2.84132	2.55586
18	3.41354	2.70398	2.37408
19	3.37683	2.72767	2.50144

**Table A.1:** The downward trend of the eigenvalues as  $M$  is increased competes with the effects of the potential well, which lowers the energy of states with small  $M$ , compared to those with large  $M$ . As  $\alpha$  is tweaked, the state minimizing the overall interaction energy (potential well and electrostatic repulsion) becomes the new ground state.

This page intentionally left blank.

# References

- [1] D. C. Tsui, H. L. Stormer, and A. C. Gossard. Two-Dimensional magnetotransport in the extreme quantum limit. *Phys. Rev. Lett.*, 48(22):1559–1562, May 1982.
- [2] R. B. Laughlin. Quantized motion of three two-dimensional electrons in a strong magnetic field. *Phys. Rev. B*, 27:3383–3389, March 1983.
- [3] R. B. Laughlin. Anomalous quantum hall effect: An incompressible quantum fluid with fractionally charged excitations. *Phys. Rev. Lett.*, 50(18):1395–1398, May 1983.
- [4] Gerald V. Dunne. Slater decomposition of laughlin states. *Int. J. Mod. Phys. B*, 07(28):4783–4813, December 1993.
- [5] B. Andrei Bernevig and F. D. M. Haldane. Model fractional quantum hall states and jack polynomials. *Phys. Rev. Lett.*, 100:246802+, June 2008.
- [6] Jainendra K. Jain. *Composite fermions*. Cambridge University Press, 2007.
- [7] E. H. Hall. On a new action of the magnet on electric currents. *American Journal of Mathematics*, 2, 1879.
- [8] M. A. Paalanen, D. C. Tsui, and A. C. Gossard. Quantized hall effect at low temperatures. *Phys. Rev. B*, 25(8):5566–5569, April 1982.
- [9] Horst L. Stormer. Nobel lecture: The fractional quantum hall effect. *Reviews of Modern Physics*, 71(4):875–889, July 1999.
- [10] Klitzing, G. Dorda, and M. Pepper. New method for High-Accuracy determination of the Fine-Structure constant based on quantized hall resistance. *Phys. Rev. Lett.*, 45(6):494–497, August 1980.
- [11] Jun-ichi Wakabayashi and Shinji Kawaji. Hall effect in silicon MOS inversion layers under strong magnetic fields. *Journal of the Physical Society of Japan*, 44(6):1839–1849, June 1978.

## REFERENCES

- [12] B. Tanatar and D. M. Ceperley. Ground state of the two-dimensional electron gas. *Phys. Rev. B*, 39(8):5005–5016, March 1989.
- [13] A. M. Chang, P. Berglund, D. C. Tsui, H. L. Stormer, and J. C. M. Hwang. Higher-Order states in the Multiple-Series, fractional, quantum hall effect. *Phys. Rev. Lett.*, 53:997–1000, September 1984.
- [14] R. G. Clark, R. J. Nicholas, A. Usher, C. T. Foxon, and J. J. Harris. Odd and even fractionally quantized states in GaAs-GaAlAs heterojunctions. *Surface Science*, 170(1-2):141–147, April 1986.
- [15] L. D. Landau. Paramagnetism of metals. *Z. Phys.*, 64:629–637, 1930.
- [16] Leslie E. Ballentine. *Quantum Mechanics: A Modern Development*. World Scientific, second edition, 2015.
- [17] V. Bargmann. On a hilbert space of analytic functions and an associated integral transform, part i. *Communications on Pure and Applied Mathematics*, 14(3):187–214, August 1961.
- [18] Brian C. Hall. *Holomorphic methods in mathematical physics*, September 2000.
- [19] R. B. Laughlin. Quantized hall conductivity in two dimensions. *Phys. Rev. B*, 23(10):5632–5633, May 1981.
- [20] Daijiro Yoshioka. *The Quantum Hall Effect*, volume 133. Springer Berlin Heidelberg, Berlin, Heidelberg, 2002.
- [21] F. D. M. Haldane and E. H. Rezayi. Finite-Size studies of the incompressible state of the fractionally quantized hall effect and its excitations. *Phys. Rev. Lett.*, 54:237–240, January 1985.
- [22] E. J. Bergholtz, T. H. Hansson, M. Hermanns, and A. Karlhede. Microscopic theory of the quantum hall hierarchy. *Phys. Rev. Lett.*, 99:256803+, December 2007.
- [23] F. D. M. Haldane. Fractional quantization of the hall effect: A hierarchy of incompressible quantum fluid states. *Phys. Rev. Lett.*, 51(7):605–608, August 1983.
- [24] N. N. Lebedev and Richard A. Silverman. *Special functions and their applications*. Dover Publications, revised edition, June 1972.
- [25] I. S. Gradshteyn and I. M. Ryzhik. *Table of Integrals, Series, and Products, Seventh Edition*. Academic Press, seventh edition, March 2007.

## REFERENCES

- [26] E. V. Tsiper. Analytic coulomb matrix elements in the lowest landau level in disk geometry. *Journal of Mathematical Physics*, 43(3):1664–1667, March 2002.
- [27] M. Kasner and W. Apel. Electrons in a strong magnetic field on a disk. *Annalen der Physik*, 506(6):433–459, 1994.